NASA CR
147502

"Made available under NASA sponsorship
in the interest of early and wide dissemination of Earth Resources Survey
Program information and without liability
for any use made thereof."

E7.6-10211

(E76-10211) COLLECTION OF RELEVANT RESULTS OBTAINED WITH THE SKYLAB IMAGES BY THE INSTITUTE FOR SPACE RESEARCH, INPE Final Report (Instituto de Pesquisas Espaciais) 95 p HC $5.00 CSCL 08B G3/43

N76-18622

Unclas 00211

SEPLAN-CNPq
Instituto de Pesquisas Espaciais - INPE
São José dos Campos - S.Paulo - Brasil

1. Classification INPE.COM 3/NTE 629.783:621.38SR	2. Period	4. Distribution Criterion
3. Key Words (selected by the author) Remote Sensing SKYLAB		internal [ ] external [X]
5. Report No. INPE-793-NTE/043	6. Date December, 1975	7. Revised by René Antonio Novaes
8. Title and Sub-title COLLECTION OF RELEVANT RESULTS OBTAINED WITH THE SKYLAB IMAGES BY THE INSTITUTE FOR SPACE RESEARCH (INPE). (FINAL REPORT)		9. Authorized by Fernando de Mendonça Director
10. Sector CRT Code 4.02		11. No. of Copies 50
12. Authorship João Botelho Machado, Antonio T. Tardin, Natalio F. Koffler, Nilton T. Higa, Hardy Jost, Renato Herz, Eric R. Stoner, José Carlos Maia, Ravindra Kumar		14. No. of Pages 90
13. Signature of first author		15. Price

16. Summary/Notes

Original photography may be purchased from:
EROS Data Center
10th and Dakota Avenue
Sioux Falls, SD 57198

Principal Investigator:

Dr. Fernando de Mendonça
Director
INPE
C.P. 515
12.200 - São José dos Campos - SP
BRASIL

NASA Headquarters Proposal Registration: 9C36

ORIGINAL CONTAINS
COLOR ILLUSTRATIONS

17. Remarks *Our Proposal to NASA (Report LAFE-171) for participating in the SKYLAB program presented three disciplines namely: Soil, Mineral and Sea Resources. In this report we show final results in only two of these disciplines and in others besides.*

TABLE OF CONTENTS

CHAPTER I

INTRODUCTION

CHAPTER I

INTRODUCTION

This final report contains a collection of information on results and findings of a few discipline investigators, working for the Brazilian Institute of Space Research (Instituto de Pesquisas Espaciais - INPE), on the earth resources studies program (SERE Program), based on data acquired during the Missions 2, 3 and 4 of the manned spacecraft SKYLAB, as intended in the document "Research and Development Proposal for Investigation Using Data from the Earth Resources Experiment Package (EREP)" of the SKYLAB, submitted to the National Aeronautics and Space Administration (NASA), Earth Observations Program Office, Office of Space Science and Applications (Report LAFE-171), in October 1971, complemented by additional information submitted, as Addenda, to the above proposal in May 1972 (Addenda to Report LAFE-171). The discipline investigators have endeavoured, under close coordination of the Principal Investigator, Dr. Fernando de Mendonça, to follow the provisions of the Statement of work for the Investigation of SKYLAB EREP Data, NASA Headquarters Proposal Registration Nº 9636", signed by the Principal Investigator in 8 March 1973.

As it is well-known, in Brazil, the responsibilities for the identification and transfer from external sources, the adaptation to national needs and limitations, and the dissemination among the users community, of the remote sensing of earth resources technology (SERE Program) have been

concentrated within the national space agency (INPE). At the very beginning of the program it was recognized that, in order to accomplish those ample objectives, the space agency had to include, in its already large range of disciplines, an in-house capability to work in all aspects of the remote sensed data interpretation employing earth sciences specialists in the various fields where the new technology is expected to provide benefits.

To this end, INPE has established, apart from its data acquiring and processing facilities and services, earth sciences interpretation teams organized under the titles of land, mineral and marine resources, geography and geodesy, and has acquired an Image-100-GE Multispectral Analyzer. This internal capability in the face of a strong outside demand of able specialists presented by an expanding market (a very desirable fact for the country as a whole), is working under quite difficult conditions, that could, in short, be described as excessively fluid in regard to the personnel component. The interpretation work force is, thus, composed of disciplinary groups integrated by a few stable investigators and a stream or flux of young university graduates under a continuous and ceaseless on-the-job and formal training, making up a combination of post-graduate university education and limited regular routine work type of operation having a fast man-power turn over rate.

In consequence, the bulk of the work with the SKYLAB data, that is being done at the INPE, is for instructional purposes, and the investigations included in the present report are not representative of

the extent of use of all the data supplied by NASA. They are simply samples thought to be relevant in the demonstration of the usefulness of the data when applied to each one of disciplines and, due to the reasons already present, and others, have the following characteristics:

With a few exceptions, the initially named co-investigators are no longer with INPE. The modified work force could not properly attend to all the objectives originally proposed and, some of the intended work could not be done for lack of a few images or problems with cloud coverage. Besides, since the original work proposal, Brazilian government priorities have changed which result is less emphasis on objectives presented in said proposal.

The data from the experimental microwave sensors, the microwave radiometer, scatterometer and altimeter, and the L-band radiometer, were not put in immediate practical use, since they were not considered significant for the on-going studies at the INPE. Therefore, interpretation efforts were concentrated on the products of the imaging sensors, specially the multispectral photographic camera and the earth terrain camera, the map of the following page shows a summary of the photographic data received.

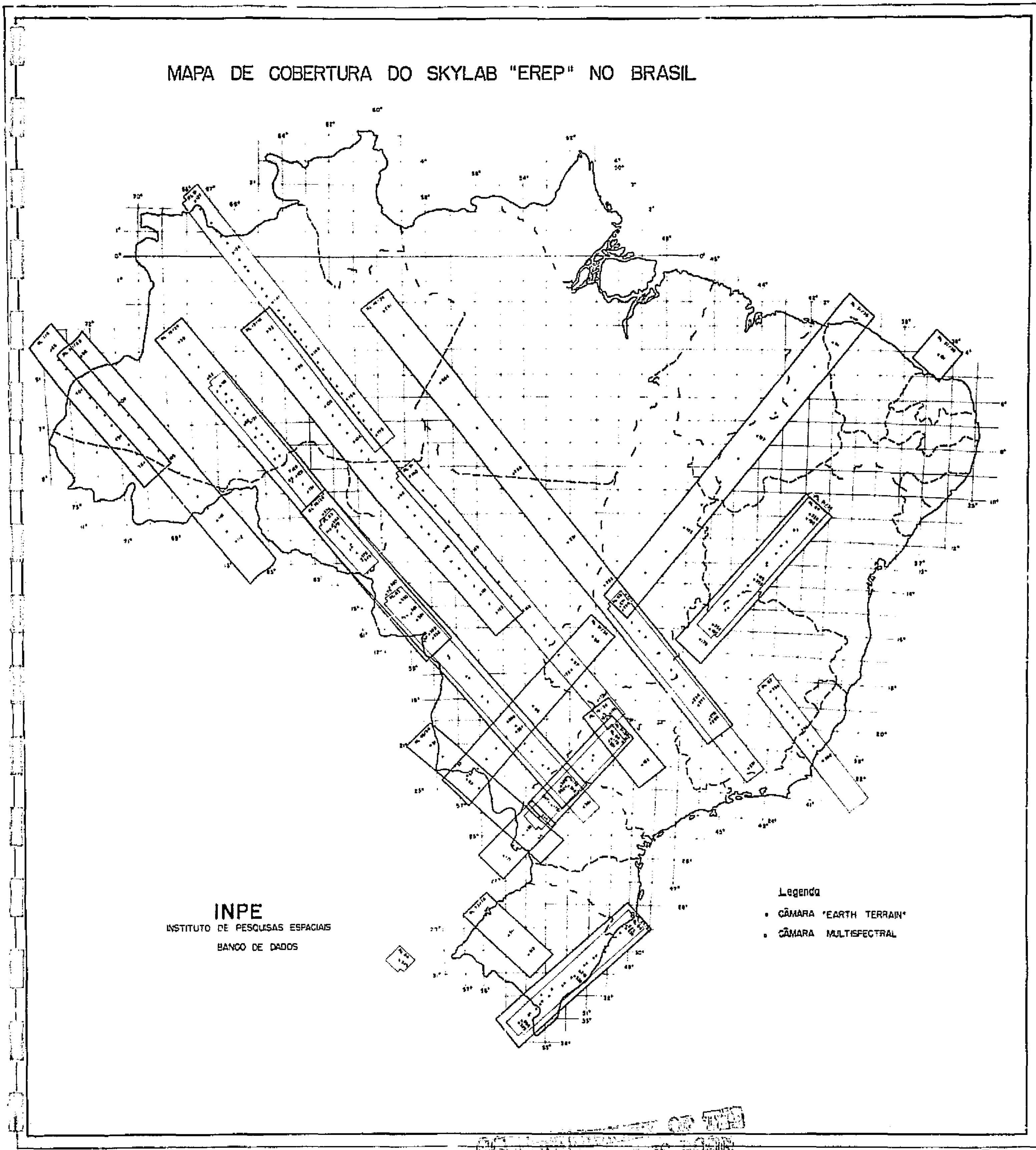

Fig. I.1 - Summary of photographic data received.

CHAPTER II

APPLICABILITY OF SKYLAB DATA TO LAND RESOURCES STUDIES

2.1 - Survey of areas occupied by coffee and wheat in Northwestern Paranã through automatic data processing of orbital imagery

prepared by:

Antonio T. Tardin

2.2 - Utilization of orbital and aircraft images in the study of soils originating from Bauru Formation sandstone

prepared by:

Natalio F. Koffler

2.3 - Evaluation of current land use in the region of Campo Grande, Mato Grosso, Brazil by analysis of SKYLAB S190A images

prepared by:

Nilton T. Higa

CHAPTER II

APPLICABILITY OF SKYLAB DATA TO LAND RESOURCES STUDIES

2.1 - SURVEY OF AREAS OCCUPIED BY COFFEE AND WHEAT IN NORTHWESTERN PARANÁ THROUGH AUTOMATIC DATA PROCESSING OF ORBITAL IMAGERY

2.1.1 - Narrative History of the Investigation

The frost which occured in July, 1975 caused severe crop damage, principally in the Northwest of the state of Paraná, Brazil. Coffee was the crop most seriously affected, with wheat also damaged to some extent.

The objective of this work was to utilize remote sensing techniques to map the coffee and wheat crops in Northwestern Paraná.

SKYLAB imagery from August 8, 1973 was used to delineate coffee growing areas. LANDSAT images obtained shortly after the frost were used to determine extent of damage in these areas, and were suplemented with partial coverage of 1:20,000 scale color infrared aerophotography and field visits.

2.1.2 - Techniques and Procedures used

Right after the frost a test area of approximately 1000 km^2 was chosen for aircraft coverage with color infrared film at a scale of 1:20,000. At the same time, field visits were made to characterize the targets under study.

Based on the results obtained by the interpretation of the aerial photographs, an analysis was made of normal color images from SKYLAB at a scale of 1:300,000 to separate areas occupied by coffee. These areas were then plotted on 1:500,000 scale LANDSAT images and served as training fields for the automatic processing of LANDSAT CCT's. Automatic processing of the LANDSAT data was carried out on General Electric's IMAGE-100 Interactive Multispectral Image Analyzer System, recently installed at INPE.

2.1.3 - Data Furnished

The SKYLAB image used was frame 361, roll 83 (Hi-Resolution Color) obtained during mission SL3 on August 8, 1973 (Fig.II.1).

2.1.4 - Results and Findings

Crops which presented well characterized patterns of coffee growing areas permitted the discrimination of the area occupied by coffee on the SKYLAB imagery (Fig.II.2).

With the field data, aircraft photographs, and SKYLAB imagery, it was possible to classify the coffee and wheat growing areas using CCT's from three LANDSAT frames by way of automatic interpretation techniques utilizing the IMAGE-100 System.

The classification results indicated 852,884 ha of frost-affected coffee, 33,864 ha of normal coffee and 302,342 ha of wheat.

This survey, briefly reported here, was a valuable contribution of remote sensing to the estimation of losses sustained by the economy of the region, on account of the frost. Since coffee still is an important component of the country's economy and the area surveyed concentrates the chief coffee plantations, the national impact of a survey of this type is of great importance.

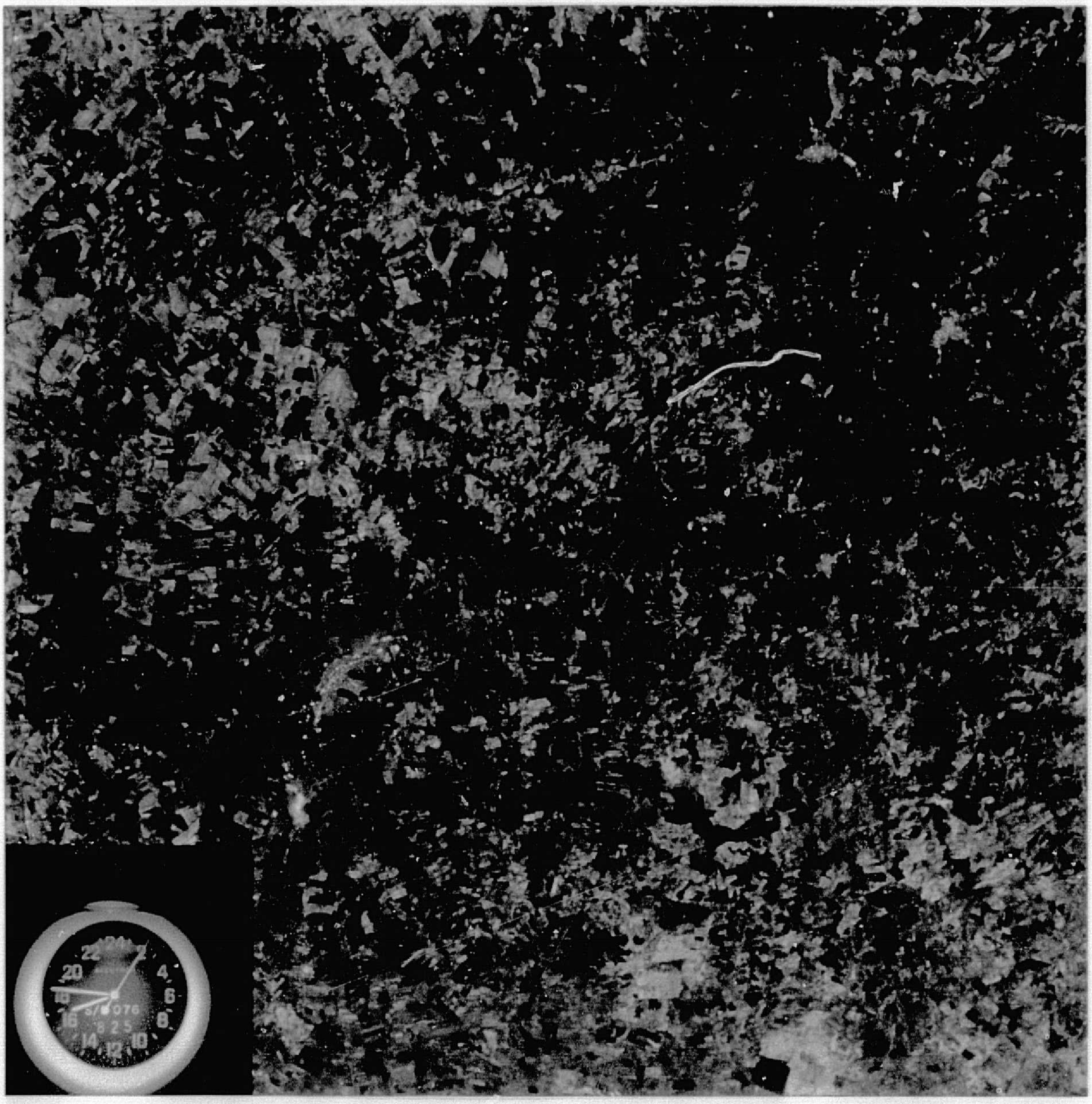

Fig. II.1 - SKYLAB SL3 images 83-360 and 83-361 (Hi-Resolution Color) obtained on August 8, 1973 near Maringá, Paraná State, Brazil (reduced from 1:300,000 scale used in study).

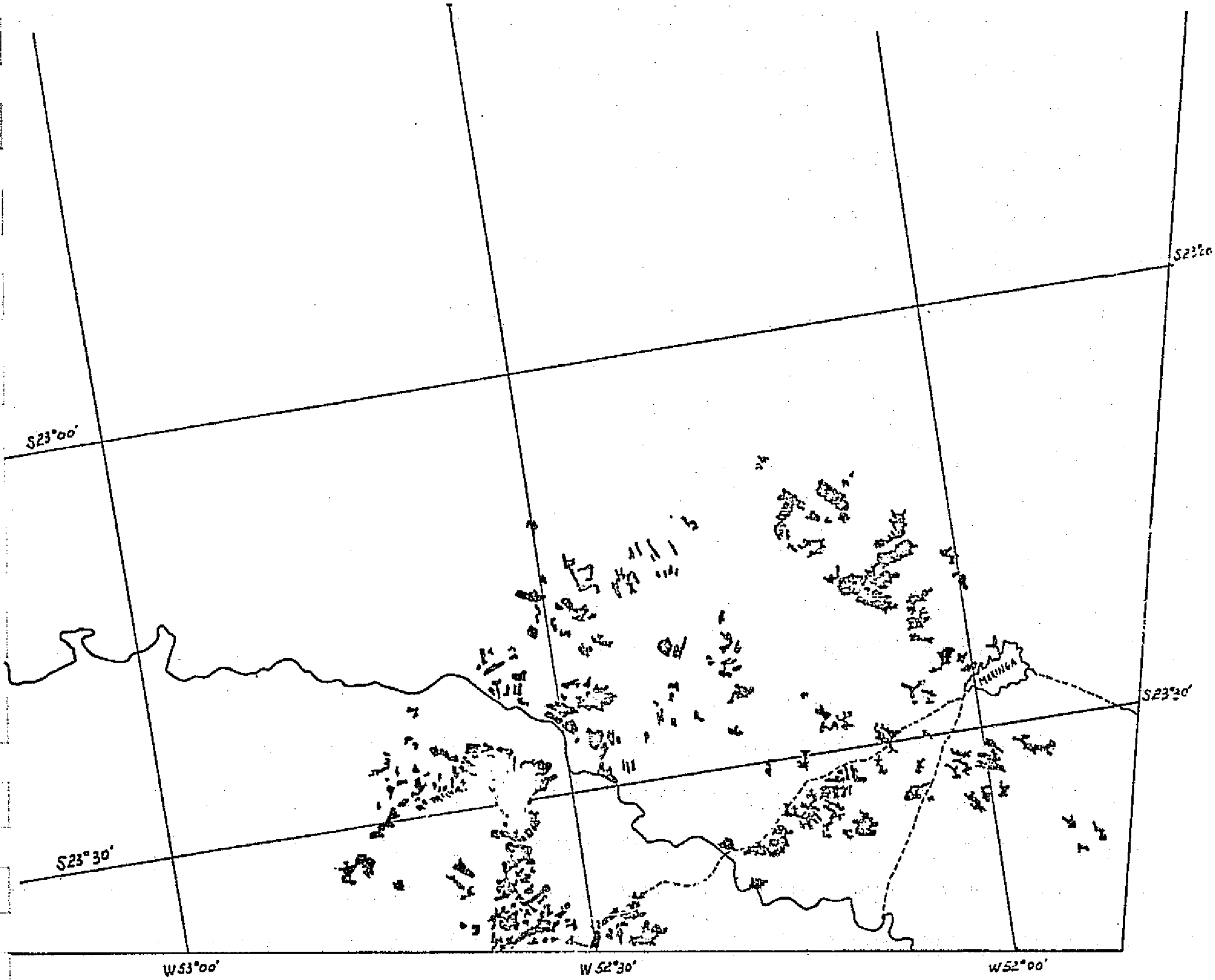

Fig. II.2 - Coffee growing areas delineated on SKYLAB image 83-361 (Hi-Resolution Color), S190B, SL3, Maringá, Paraná State, Brazil.

2.2 - UTILIZATION OF ORBITAL AND AIRCRAFT IMAGES IN THE STUDY OF SOILS ORIGINATING FROM BAURU FORMATION SANDSTONE

2.2.1 - Narrative History of the Investigation

The purpose of this study was to characterize drainage pattterns in soils derived from Bauru sandstone through conventional techniques of photointerpretation. Descriptive and quantitative parameters of soil drainage patterns were obtained from analysis of orbital and aircraft imagery. Imagery utilized included LANDSAT and SKYLAB images (1:500,000 scale) and aircraft images (1:60,000 and 1:25,000 scale).

2.2.2 - Techniques and Procedures used

Circular samples of drainage patterns were taken from the images to characterize the following drainage parameters: drainage density, frequency of rivers, texture ratio, and topographic texture. The area of the circular sample varied according to the image scale. The 1:25,000 scale aircraft images were sampled by 10km^2 circular areas, while the 1:60,000 scale aircraft images were sampled by 20 km^2 circular areas. The 1:500,000 scale orbital imagery was sampled by 100 km^2 circular areas.

2.2.3 - Data Furnished

Photographic images were obtained from the September 4,1973

pass of SKYLAB SL3 over western São Paulo state, Brazil (Figs. II.3 and II.4). Images from the following sensors were used in this study:

1. Sensor S190-A (Multispectral Photographic Camera)
   a. Identification Nº: frame 178, roll 35
   b. Film Type: SO-022 (Panatomic-X, Black and White)
   c. Spectral Band: (0.6-0.7 μm)
   d. Scale (approx.): 1:500,000
   e. Format: 32.6 x 32.6 cm print
   f. Area covered: 26,000 km^2

2. Sensor S190-B (Earth Terrain Camera)
   a. Identification Nº: frames 349 and 350, roll 84
   b. Film Type: SO-242 (Hi-Resolution Color)
   c. Spectral Band: (0.4 - 0.7 μm)
   d. Scale (approx.): 1:500,000
   e. Format: 22.5 x 22.5 cm color transparency
   f. Area covered: 12,000 km^2

2.2.3 - Results and Findings

The drainage network was traced over the SKYLAB images in a detailed manner, and 100 km^2 circular samples were taken representing the two great groups of soil in the area: Dark Red Latosol (sandy phase), and Lins and Marília Podzols.

This analysis verified that even with the small scale of the SKYLAB images it was possible to characterize the two great groups of soil: Differences in soil drainage patterns traced from SKYLAB image 84-350 allowed the delineation of boundaries between the two soils (Fig. II.5). Aircraft and orbital imagery proved useful in obtaining discriminatory parameters of soil drainage patterns which served to characterize the soil units being studied.

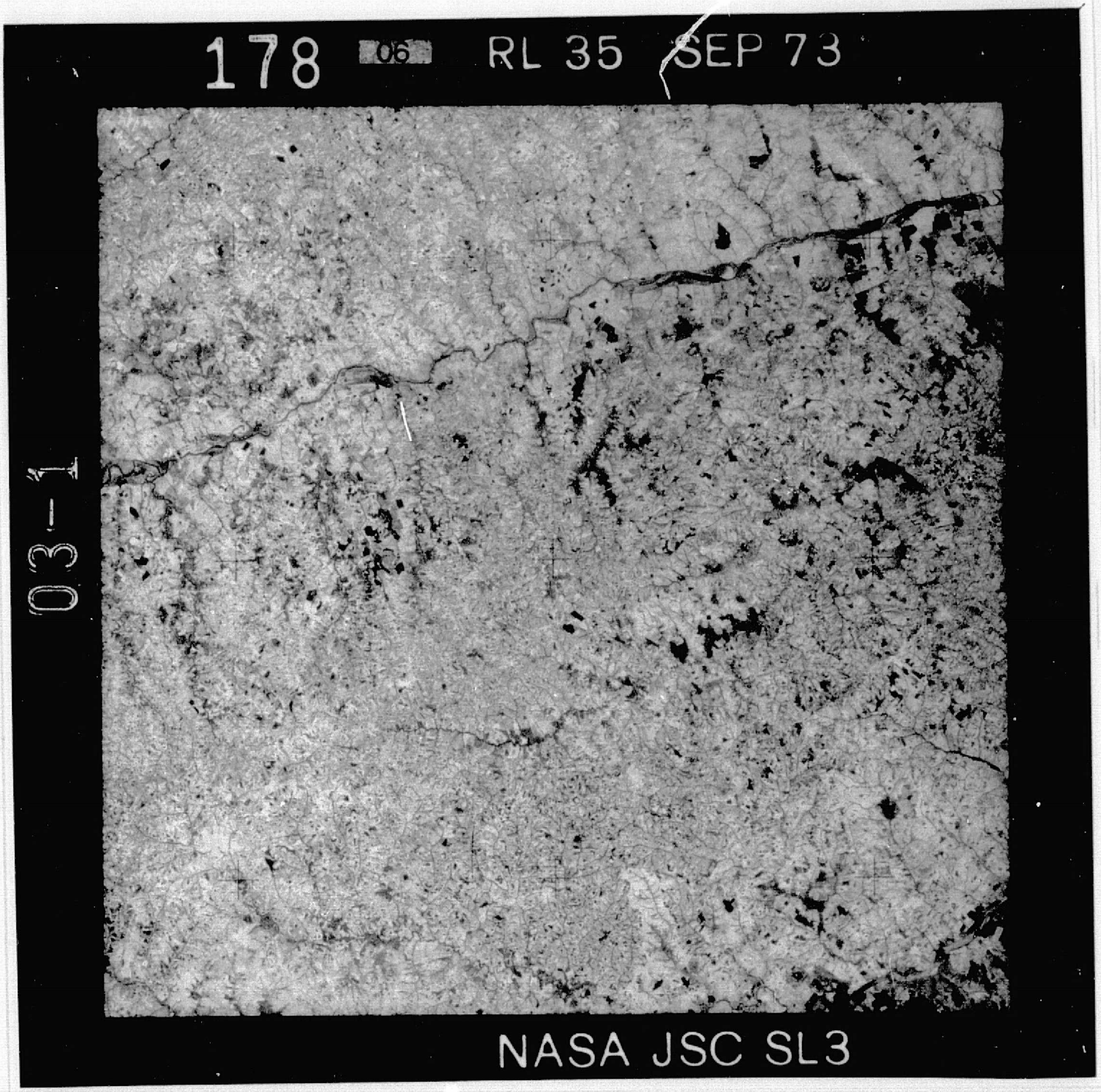

Fig. II.3 - SKYLAB SL3 image 35-178 (Panatomic-X,B&W) obtained September 4, 1973 over western São Paulo State, Brazil (reduced from 1:500,000 scale used in study.)

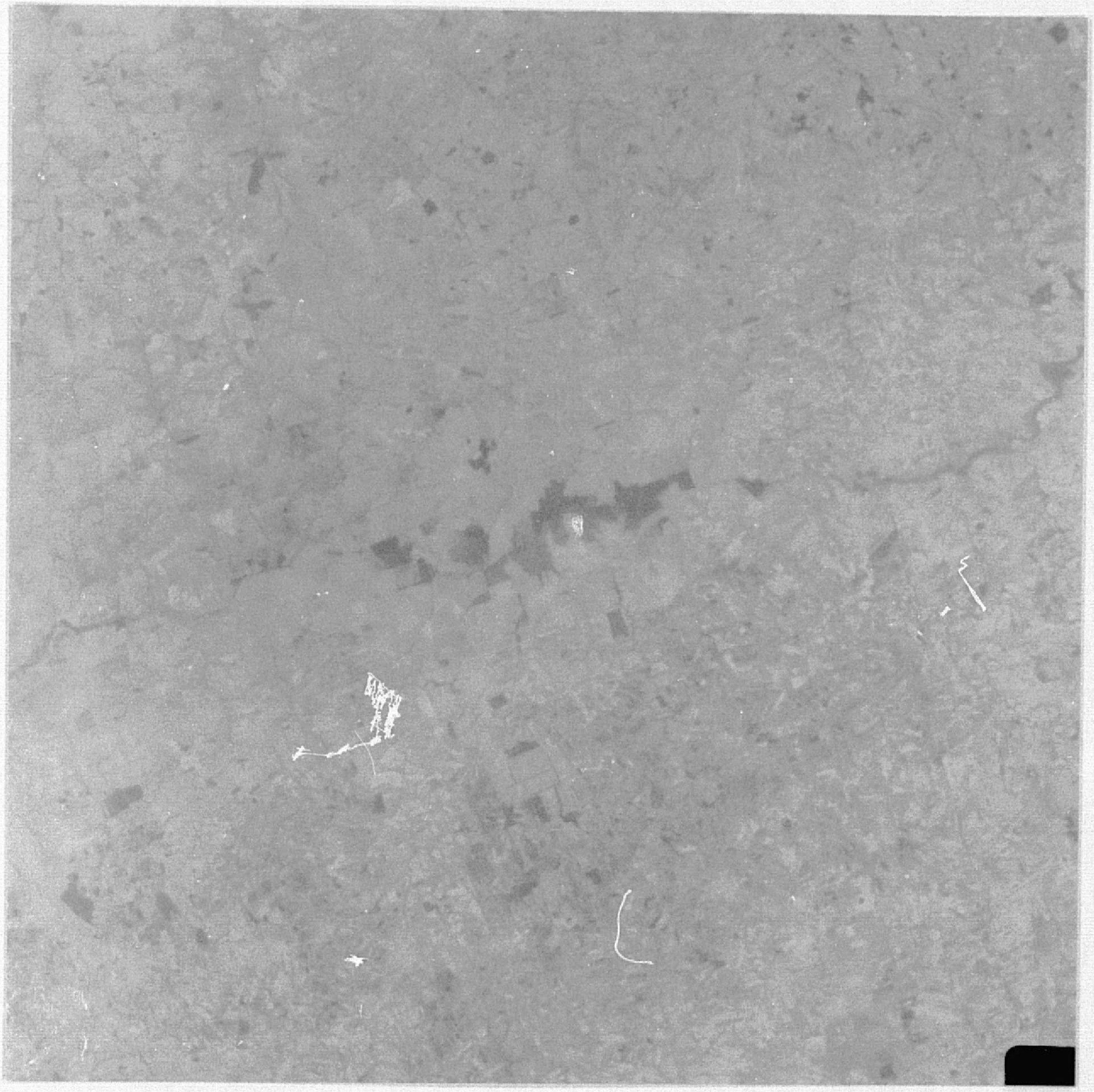

Fig. II.4 - SKYLAB SL3 image 84-350 (Hi-Resolution Color) obtained September 4, 1973 over western São Paulo State, Brazil (reduced from 1:500,000 scale used in study).

2.3 - EVALUATION OF CURRENT LAND USE IN THE REGION OF CAMPO GRANDE, MATO GROSSO, BRAZIL, BY ANALYSIS OF SKYLAB S190A IMAGES

2.3.1 - Narrative History of the Investigation

Two photographic images from the September 3, 1973 pass of SKYLAB SL-3 over southern Mato Grosso state, Brazil were utilized to study current land use patterns. The study area is centered on the city of Campo Grande, Mato Grosso and takes in an area of 26,561 km^2 (Fig. II.6).

2.3.2 - Techniques and Procedures used

Conventional photointerpretation techniques were used to transfer information from the images to a transparent overlay. Area was measured using a grid in which the smallest element had an area of one millimeter square.

2.3.3 - Data furnished

The two photographic images utilized were obtained from sensor S 190-A and are identified as follows (Figs. II.7 and II.8)

Roll	Frame	Station	Film Type
33	93	3	EK-2443 (Color IR)
34	93	4	SO-356 (Hi-Resolution Color)

2.3.4 - Results and Findings

Eight classes of soil use were separated and mapped (Fig.II.9):

1) Small scale
   agricultural areas - principally in areas of high soil fertility close to Campo Grande.
2) Large scale agricultural areas-predominantly extensive plantations of rice, soybeans, and wheat.
3) Cleared pasture land with little remaining native vegetation.
4) "Cerrado" vegetation - low scrub tree and brush formation.
5) "Cerradão" vegetation - scrub forest formation.
6) Forest vegetation - occurs in isolated spots in association with "Purple" Latosol (Latosolo Roxo).
7) Native rangeland - used principally as pasture land, but may undergo cultivation in some areas.
8) Burned areas.

Area occupied by each class was calculated and the percentage relative to the total area expressed for the eight classes (Table II.1).

It was possible to delineate seven suitability classes, indicating the extent of human exploration of the region (Fig.II.10).

1) Areas with intensive agricultural activity with large scale plantations predominant.
2) Areas with intensive agricultural activity with small scale plantations predominant.
3) Forest areas with little exploration.
4) Cleared pasture land, intensively explored by man.
5) Areas of "cerradão" (scrub forest) vegetation with little indication of human exploration.
6) Areas of "cerrado" (low scrub tree and brush) vegetation with little human exploration.
7) Areas with varying topography and predominant "cerradão" vegetation with little human utilization.

The data interpretation confirmed that the intensity of agricultural exploration coincided with soils of good quality. Natural vegetation predominated in the region, while forest clearing appeared not to be intensive. The practice of burning pasture and crop land appeared to be carried out in an indiscriminate manner, even in intensively cultivated areas of good soil quality.

TABLE II.1

AREA OF EACH CLASS OF SOIL USE AND ITS PERCENTAGE RELATIVE TO THE AREA STUDIED

SOIL USE CLASS	AREA (ha)	PERCENTAGE AREA
Cerrado Vegetation	760,278	28.62
Cerradão Vegetation	425,435	16.01
Forest Vegetation	410,854	15.46
Large Scale Agriculture	409,936	15.42
Small Scale Agriculture	171,918	6.47
Native Rangeland	158,504	5.96
Cleared Pasture Land	86,468	3.25
Burned Areas	38,775	1.46

LEa - Dark Red Latosol (Sandy Phase)
PLM - Lins and Marília Podzols

Fig. II.5 - Soil drainage patterns traced from SKYLAB image 84-350 (Hi-Resolution Color), S190-B, SL3, western São Paulo State, Brazil with soil great group boundaries delineated.

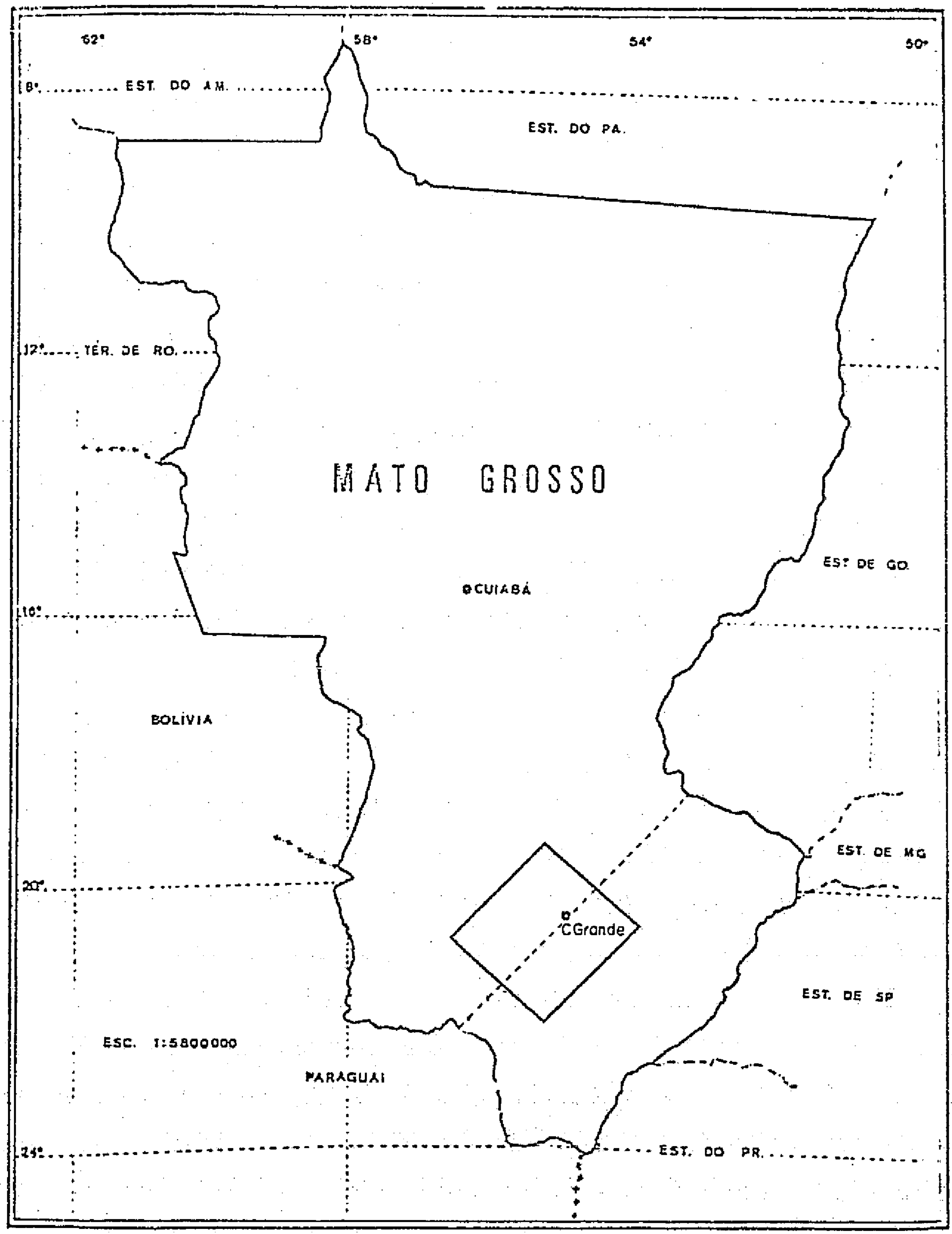

Fig. II.6 - Location of study area.

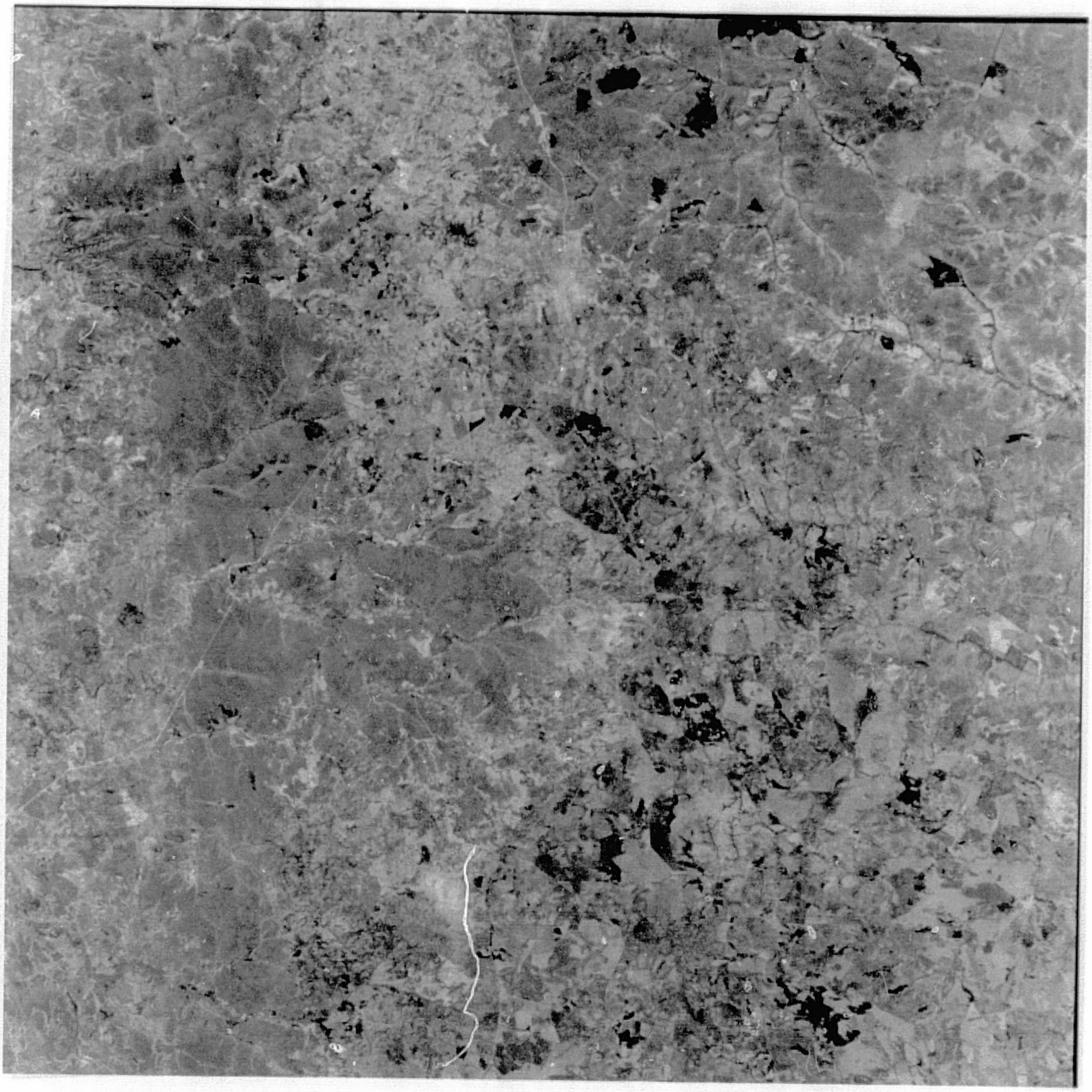

Fig. II.7 - SKYLAB SL3 image 33-93 (Color IR) obtained September 3,1973 over Campo Grande, Mato Grosso state, Brazil (reduced from 1:500,000 scale used in study)

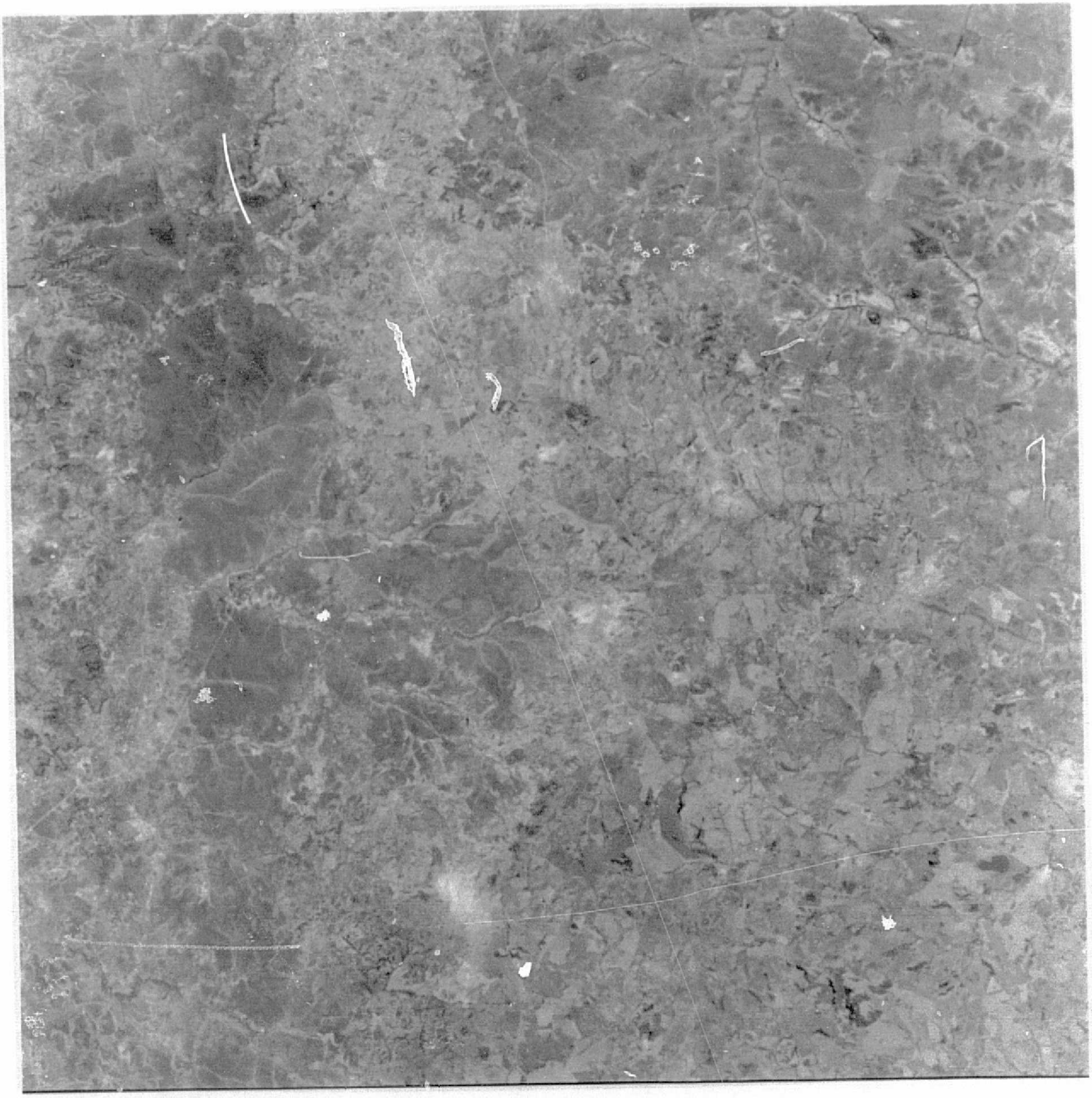

Fig. II.8 - SKYLAB SL3 image 34-93 (Hi-Resolution Color) obtained September 3, 1973 over Campo Grande, Mato Grosso state, Brazil (reduced from 1:500,000 scale used in study).

The following figure (Fig. II.9) is a map of current soil use in the region of Campo Grande, Mato Grosso State, Brazil based on interpretation of SKYLAB SL3 S190 A images 33-93 (Color IR) and 34-93 (Hi-Resolution Color).

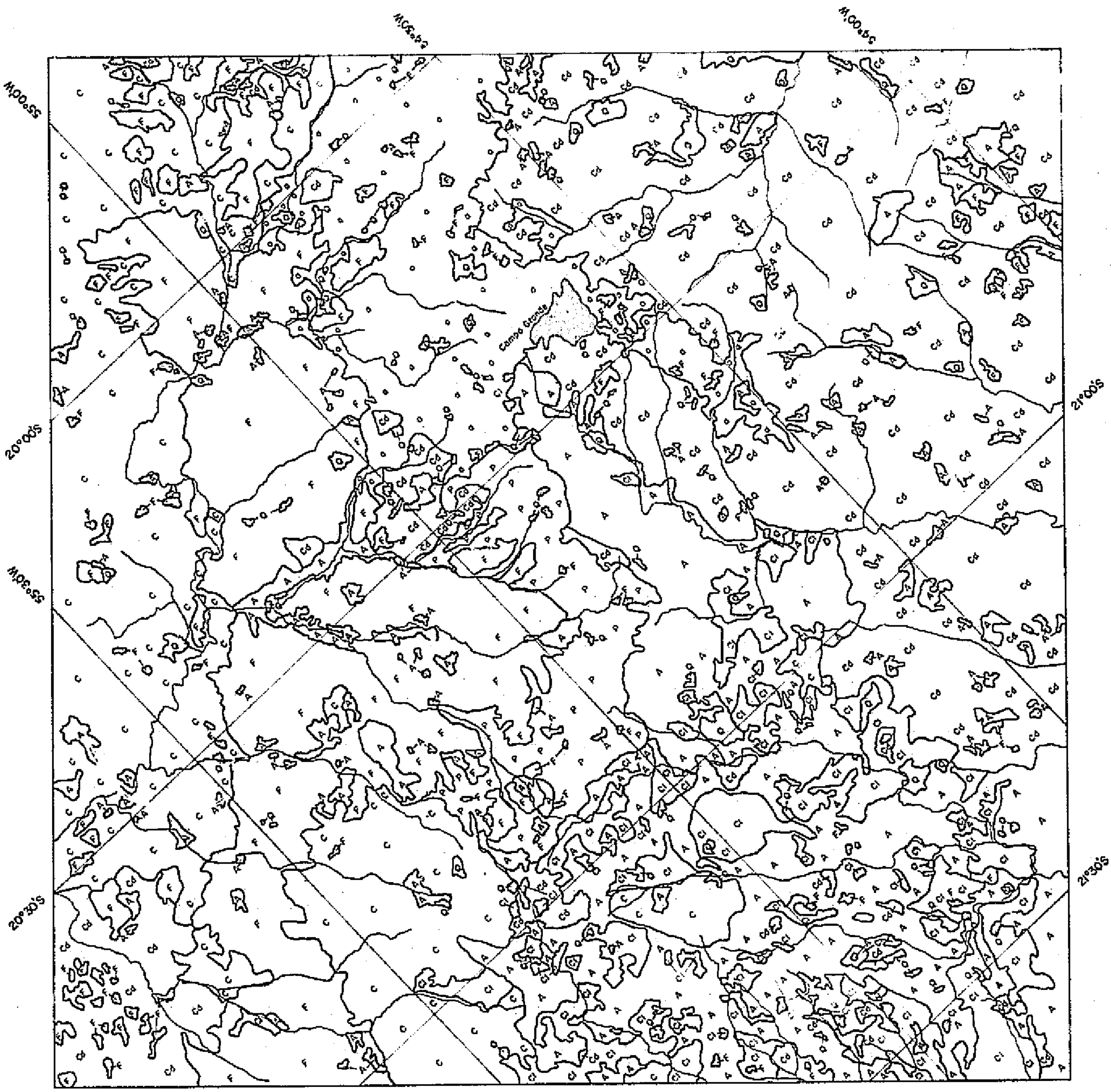

Fig. II.9 - Map of current soil use in the region of Campo Grande, Mato Grosso State, Brazil based on interpretation of SKYLAB SL3 S190A images 33-93 (Color IR) and 34-93 (Hi-Resolution Color).

LEGEND

a - Small scale agricultural areas.
A - Large scale agricultural areas.
P - Cleared pasture land.
Cd - "Cerrado" vegetation.
C - "Cerradão" vegetation.
F - Forest vegetation.
Ci - Native rangeland.
B - Burned areas.

The following figure (Fig. II.10) is a map of soil suitability in the region of Campo Grande, Mato Grosso state, Brazil based on interpretation of SKYLAB SL3 S190A images 33-93 (Color IR) and 34-93 (Hi-Resolution Color).

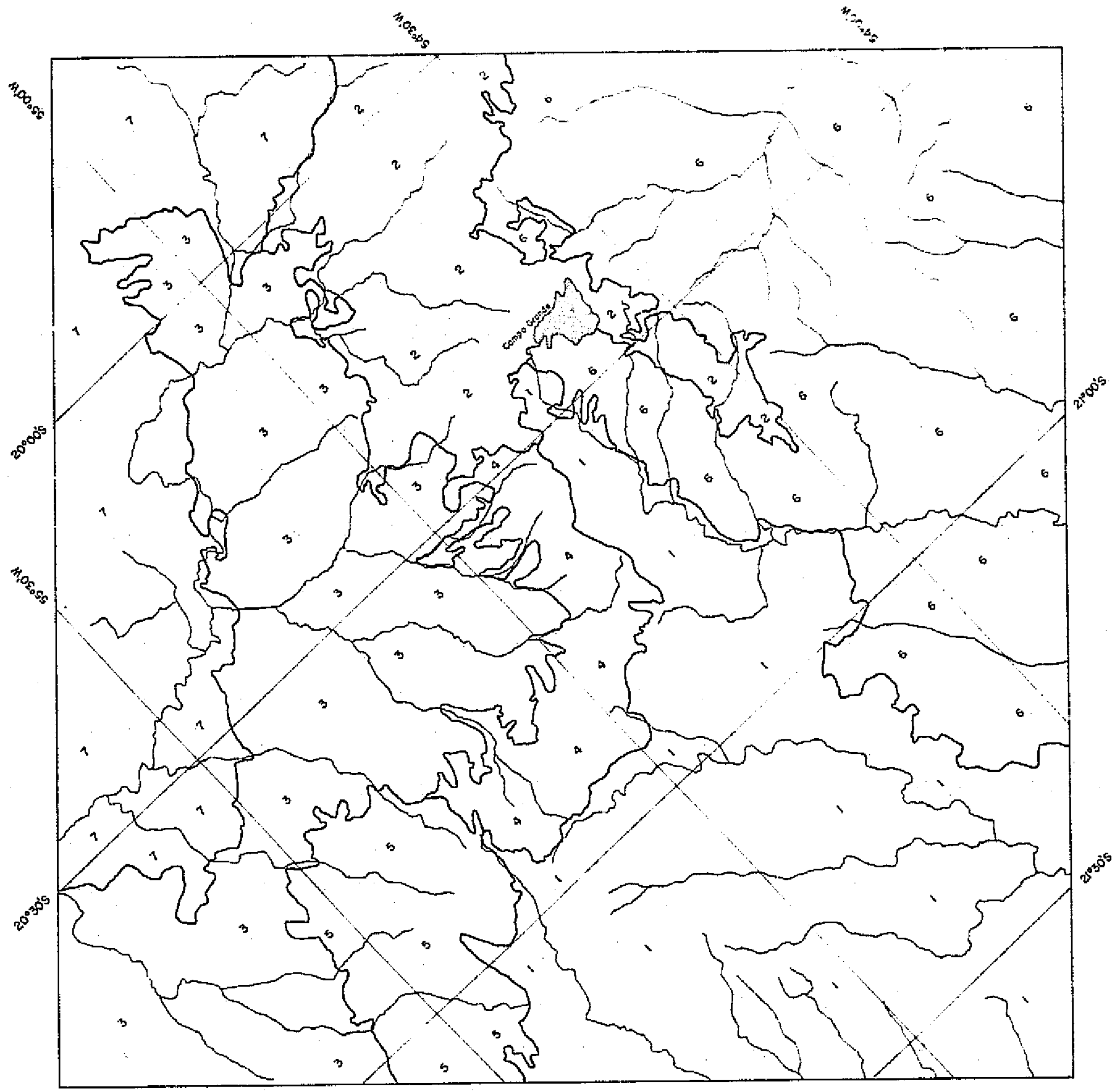

Fig. II.10 - Map of soil suitability in the region of Campo Grande, Mato Grosso State, Brazil based on interpretation of SKYLAB SL3 S190A images 33-93 (Color IR) and 34-93 (Hi-Resolution Color).

LEGEND

1 - Areas with intensive agricultural activity with large scale plantations predominant.
2 - Areas with intensive agricultural activity with small scale plantations predominant.
3 - Forest areas with little exploration.
4 - Cleared pasture land, intensily explored by man.
5 - Areas of "cerradão" vegetation with little human exploration.
6 - Areas of "cerrado" vegetation with little human exploration.
7 - Areas with varying topography and predominant "cerradão" vegetation with little human utilization.

CHAPTER III

APPLICABILITY OF SKYLAB DATA TO QUATERNARY COASTAL STUDIES

Prepared by:

Hardy Jost

Renato Herz

CHAPTER III

APPLICABILITY OF SKYLAB DATA TO QUATERNARY COASTAL STUDIES

3.1 - NARRATIVE HISTORY OF THE INVESTIGATION

Until 1973 the state of knowledge of the physical factors which govern the distribution of water masses along the coastal plain of Rio Grande do Sul (SE-Brazil) were based only on data collected by classical oceanographic methods.

By that time, the Remote Sensing Program of the Institute of Space Research (INPE) began to use orbital imagery to establish its resolution capability in studying hydrological and oceanographic conditions in that area (Herz, 1973). The immediate interest in the application of such a methodology to oceanography lies in the repetitive and synoptic nature of the surveying over large areas.

Remote sensing techniques in use by INPE's staff, together with conventional oceanographic methods, are creating new possibilities for discovering the main physical elements which control the circulation patterns in surface waters of that coastal area.

The analysis of research under development both at INPE and at the Geology Department of the Federal University of the State of Rio

Grande do Sul (UFRGS), favored the combining of efforts in the study of physical control factors which govern water circulation along with the geological framework established mainly by the Quaternary coastal deposits. A project was then proposed to INPE to study the sedimentary and morphological evolution of the coastal plain (mainly those disposed around the Patos Lagoon), the main hydrological feature of that region, and establish whatever control is exerted by that evolution on the actual morphology and water circulation.

In this paper we will make an attempt to depict the resolution capacity of orbital imagery for studies of coastal areas and to establish the degree of influence of prior geometries of emerged areas of Quaternary age on actual geometrical properties of lagoonal systems. With these objectives in mind, we tried to delineate the major well known Quaternary outcroping stratigraphic units and reconstruct the paleogeographic evolution of the area. Our work was based upon numerous and consistent data collected during the last eight years as ground truth stored at UFRGS by the Quaternary Studies group.

While the hydrological studies were being made through the interpretation of LANDSAT-1 MSS imagery for the purpose of stratigraphic unit identification, the images from SKYLAB SL-3 mission on September 1st, 1973 were used (Fig. III.1).

The selected images cover the whole extent of the test

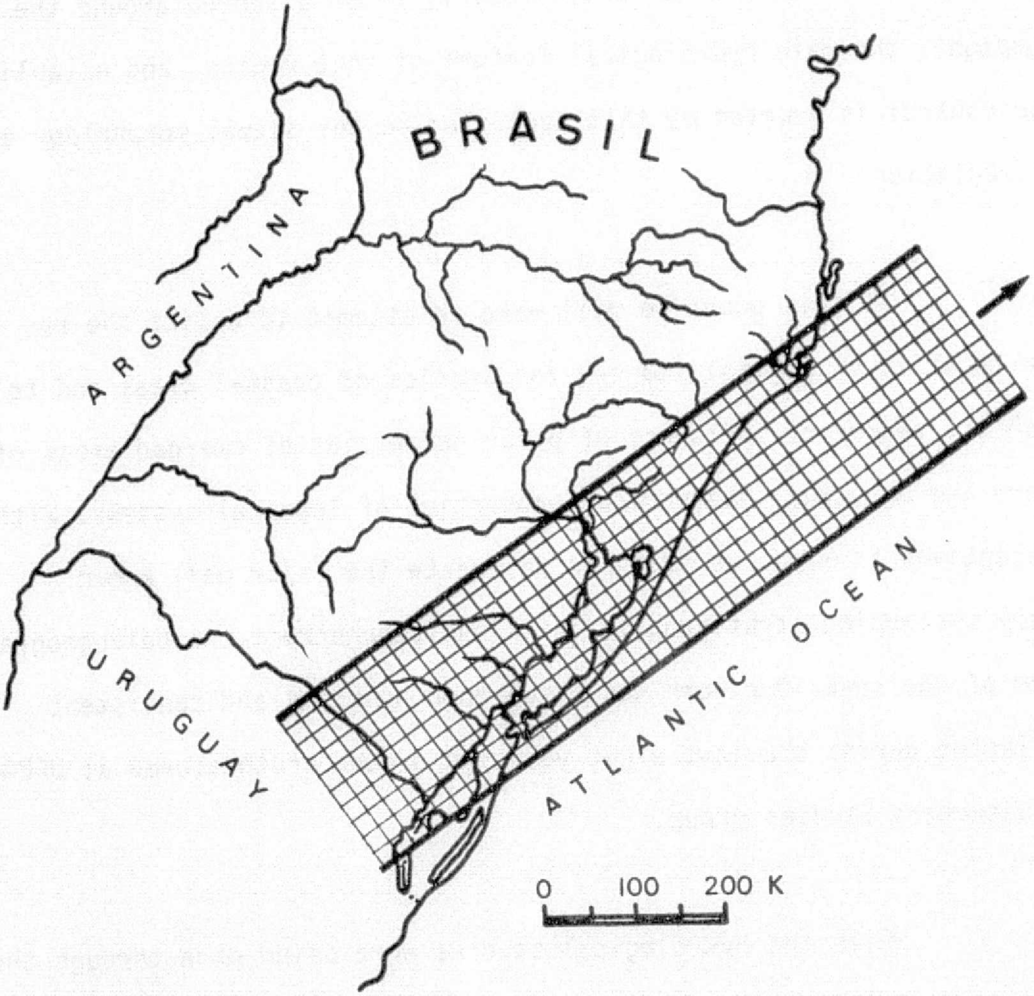

Fig.: III.1 - SKYLAB SL-3 Ground Track on 1st. Sept. 1973.

area, starting at 29°00' latitude south with their southern limits at latitude 32°30' south (Fig. III.2).

It should be emphasized that while LANDSAT-1 imagery is repetitive and synoptic, the available SKYLAB images are not. Therefore, effects of different climatic conditions on surface feature response could not be evaluated on multispectral images.

3.2 - TECHNIQUES AND PROCEDURES USED

The sensors used in the SKYLAB SL-3 manned orbital mission comprise the following systems: the S-190A multispectral photographic camera, the S-190B earth terrain camera for high resolution photography in support of other Earth Resources Experimental Package (EREP) systems, the S-191 infrared spectrometer, the S-192 Multispectral Scanner, the S-193 radiometer-scatterometer-altimeter and the S-194 L-Band radiometer.

To fulfill the objectives of this paper, imagery taken by the S-190A multispectral camera was used, consisting of images from six high-precision photographic cameras centered on the same ground point. The syncronism between spacecraft velocity and rate of imaging was adjusted during the flight to obtain a longitudinal overlap of about 60%.

The expected ground resolutions for the S-190A standard film/filter combinations (at a contrast ratio of 6.3 to 1) are as follows (NASA, 1974).

The following figure (Fig.III.2) is a photomosaic of the Lagoa dos Patos in southern Brazil, using SKYLAB imagery of September 1st, 1973.

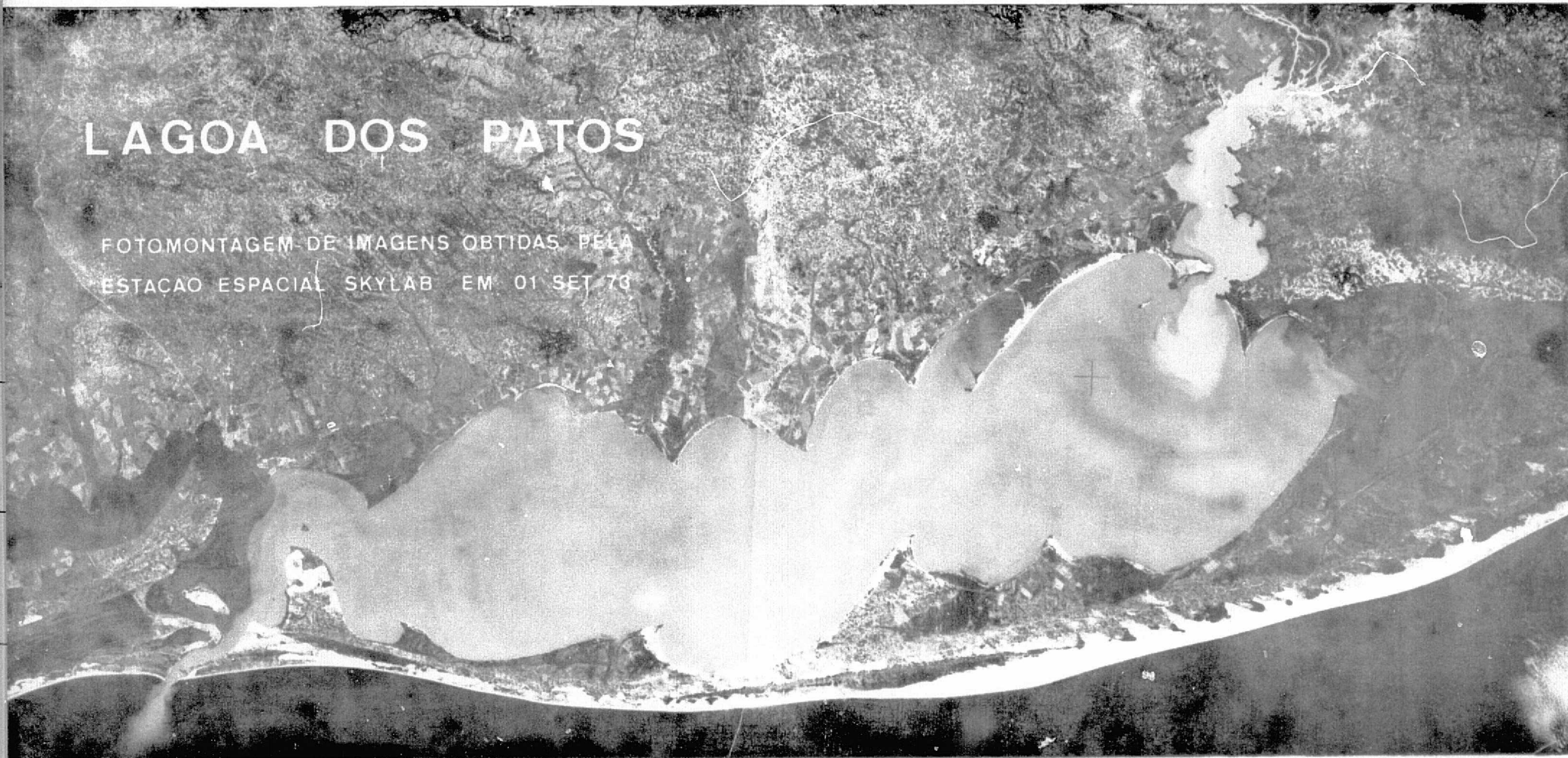
LAGOA DOS PATOS
FOTOMONTAGEM DE IMAGENS OBTIDAS PELA
ESTAÇAO ESPACIAL SKYLAB EM 01 SET 73

WAVELENGTH MICROMETERS	FILM	ESTIMATED GROUND RESOLUTION IN m.	STATION
0.5 - 0.6	PAN-X B&W (SO022)	40-46	6
0.6 - 0.7	PAN-X B&W (SO022)	30-38	5
0.7 - 0.8	IR B&W (EK2424)	73-79	1
0.8 - 0.9	IR B&W (EK2424)	73-79	2
0.5 - 0.88	IR color (EK2443)	73-79	3
0.4 - 0.7	HIR color (SO356)	40-46	4

Within these general spectral regions, various film/filter combinations were used. The spectral regions designated were selected to separate the visible and photographic infrared spectrum into bands that were expected to be most useful in multispectral analysis. The selection was based upon the experience gained in the NASA Earth Observations Aircraft Program, the performance of Apollo experiment S-065, and other multispectral photographic studies that have been performed to date.

3.3 - DATA DISCUSSION

In regions of sparse vegetation, which is the case of the chosen test area, good geologic reconnaissance maps can often be prepared from orbital imagery where distinctive outcrop patterns occur. Sometimes these maps are superior to ground-based geological maps since contacts may

be better delineated in the overview."Remote sensed units" are depicted, rather than formal lithological or stratigraphical units, at least until field cheking demonstrates a correlation between the two categories.

Orbital images, especially in mosaic form, provide an excellent means of landform analysis and regional geomorphologic mapping. In this way, successful studies have been done on this subject in many regions of the world, mainly based on LANDSAT-1 imagery.

The construction of a geologic map is based upon the distribution of the remote sensing mapping units identified and outlined on the imagery. In general, the methodology used is very similar to that used for conventional photogeologic interpretation. The sharpness of a boundary depends mainly upon the different resistances to erosion between two or more units (petrovariance or morphologic hardness). The delineation of a boundary is limited to visible features and the ability to follow it depends upon the continuity expressions of the image for a given feature.

Distinctive differences in drainage pattern, different density of vegetation cover, different types of soil with which vegetational zones may or may not be associated and contacts between depositional and erosional areas, are features which can usually be identified on the imagery in tonal contrasts.

Identification of stratigraphic units from LANDSAT is

impossible in most cases because of the low linear resolution capability of the multispectral system (70-100 meters), the absence of stereoscopic vision and the small scale.

3.4 - INTERPRETATION OF S-190A MULTISPECTRAL BANDS

An analysis of SKYLAB multispectral images was first made in such a way as to evaluate the image resolution capability in the recognition and mapping of known surface units of Northern Rio Grande do Sul coastal plain. The results gained from this initial analysis are as follows:

STATION 6 - Wavelength 0.5-0.6 micrometers (filter-green to orange). Tonal contrast is weak. Water bodies show uniform dark gray to light gray tones; some of them are not clear and sometimes they cannot be distinguished from dense vegetation zones. Drainage patterns are shown but not clearly. Sand bodies are visible but with a lower resolution than on band 5. Terraces are visible but only weakly distinguishable. Pediments are untraceable. Topographic lineaments are not clear. Marshy ponds cannot be identified. Narrow beaches, close to sand dunes, are not visible. "Remote sensed units" are very difficult to trace.

STATION 5 - Wavelength 0.6-0.7 micrometers (filter-orange to red). Tonal contrast is good. Boundary of water is very sharp

and can be easily outlined; some of them are still not clear inside dense vegetation zones. Drainage patterns are well defined. Limits of sand bodies are easily traced. Minor holocene water deposited features are obscured and sometimes difficult to trace or identify.Band 4 has better resolution for these features. Terraces can be easily traced. Pediments can be identified and traced. Topographic lineaments are clearly shown. Marshy ponds can be identified but some of them with difficulty. Narrow beaches near dunes are still not identifiable. A great number of"remote sensing units" can be distinguished and their boundaries traced.

STATION 1 - Wavelength 0.7-0.8 micrometers (filter-red-to near infrared). Tonal contrast is poor. Water bodies appear clearly. Drainage pattern is obscured. Some channels are shown clearly, mainly the widest rivers. It can be used for mapping Quaternary sediment deposits because this band, as in band 7, offers a sharp response to high moisture content. This difference in reflectance, caused by absorption of this wavelength, clearly delineates between Holocene and Pleistocene deposits. Sand dunes bodies of Pleistocene age are dull and their limits cannot be traced, but Holocene dunes are still very clear. Pediments are untraceable. Topographic lineaments can be examined. Marshy environments cannot be distinguished from water bodies.

Narrow beaches close to dunes can be traced but with some difficulties and the same can be said with respect to humid sand bodies inside dune belts.

STATION 2 - Wavelength 0.8-0.9 micrometers (filter-IR). Tonal contrast is poor. Water bodies appear very clear and main river courses are shown clearly, but the drainage pattern is rather obscured. Some wide sedimentary structures both in Pleistocene and Holocene deposits are not shown in other bands, appear in this one. Boundaries between Quaternary units can be traced, but with some difficulties. Details inside Holocene dunes are visible and beaches close to dunes are easily traced. Topographic lineaments can be examined. Pediments are untraceable.

STATION 4 - Wavelength 0.4-0.7 micrometers (filter EE)-high resolution color emulsion used to control multispectral analysis.

3.5 - RESULTS AND FINDINGS

The interpretation of the SKYLAB S-190A imagery allowed the recognition according to their morphological expression, linear features, tonal contrast, water table position, photographic texture and reflectance in each multispectral channel.

In spite of their diversity, it was possible to group all

units into two main kinds which comprise morphological and stratigraphic units.

3.5.1 - Morphological Units

The morphological units of the coastal plain of the State of Rio Grande do Sul, considering only the low-lying flat area around the Patos Lagoon, can be divided into accumulation forms and erosional forms.

Accumulative forms were identified by the use of single criteria proposed by Zenkovich (1967) to coastal features. They were considered according to their shape, the nature of their connection with higher lands, orientation relative to the elements of the coast (on the open coast or inside the lagoons), their secondary morphological features like curvature, extent and direction of curvature, and presence and size of hook-shaped bends. Dynamically, the accumulative forms were considered from the point of view of the stable and mobile forms, growth mechanisms, place and level of development, relative vertical movements, and contemporary activity like overspilling of waves. Genetically, the main process in the supply of material: sources of supply, causes of accumulation, dependance of forms (primary,secondary on top of primary, and induced forms), and stage of development (rudimentary, completely developed, decaying, relict or regenerated), were taken into account.

All forms were considered from three points of view: whether

their formation was linked to aeolian effects, wave effects, or current (river) action.

According to these criteria, the SKYLAB imagery of the coastal test area under investigation showed to be very useful and allowed for the identification of a great number of both accumulative and erosional forms, either recent or old ones, and of variable size, including small features of not more than 500 meters in length.

The following forms were identified and are still under study:

1) Accumulative Forms

i) Wave action forms

a) attached

- beaches
- wave-built terraces both on smooth and projecting sectors of the lagoon, and infilling indentations.
- assymetrical (simple), rounded and cuspate forelands.
- beach-dune-ridge belts and crests.

b) free forms

- spits, as simple forms fed only from one direction, continuing the line of the original strand line and curving into bays.

c) barrier - as the main form of accumulation in the coastal plain. The barrier is actually a complex one, formed by action of multiple processes since upper Pleistocene. It is actually assymetrical, rounded on the sea face and fed only in the internal lagoonal face.

d) detached forms - represented by small accumulation islands, doubtfully relict forms or in course of formation inside the lagoons.

ii) Aeolian forms

Long-shore built dune belts could be identified, both recent and fossilized. Fossil dunes have been related to high sea-levels of Pleistocene age in this area (Jost, 1971). In decreasing order of occurrence, transversal barchan dunes, climbing dunes and isolated parabollic dunes were recognized. Barchan dunes built up the recent field lying close to the sea-shore, while the climbing dunes comprise extensions of those dunes which gently and partially cover wave-cut terraces built on Pleistocene terrains. Parabolic dunes are shown well in the images as inverse transversal barchan-shaped and isolated sand bodies.

iii) River current action forms

a) Deltaic deposits:

- Bird-foot deltas like the Jacui river mouth
- Arched beach-ridged deltas like the Camaquã river

b) Fluvial sand ridges associated with meander processes

c) River terraces

d) Apparent current drowned river mouths

2) Erosional Forms

i) Wave-cut terraces of regional expressions, namely former erosional cliffs constructed on older coastal sediments

ii) River cut terraces

iii) Aeolian blow-out spots

3.5.2 - Stratigraphic Units

Several lithostratigraphic units which occur at the surface of the test area could be identified in the imagery and their regional distribution can be followed in figure III.3. These units comprise:

1) Unit A

This unit comprises discontinuous deposits related to post-Wisconsin high sea level stand. These deposits are the result of the existence of several sub-aqueous environments which existed during the last 6,000 years of coastal evolution. Known as Quinta Transgression (Jost & Godolphim, 1975), the late Holocene high sea-level favored the development of the following recognizable environments:

The following figure (Fig. III.3) presents the Rio Grande do Sul coastal plain stratigraphic units, (based on SKYLAB SL-3, S-190A multispectral images taken in September 1st, 1973.

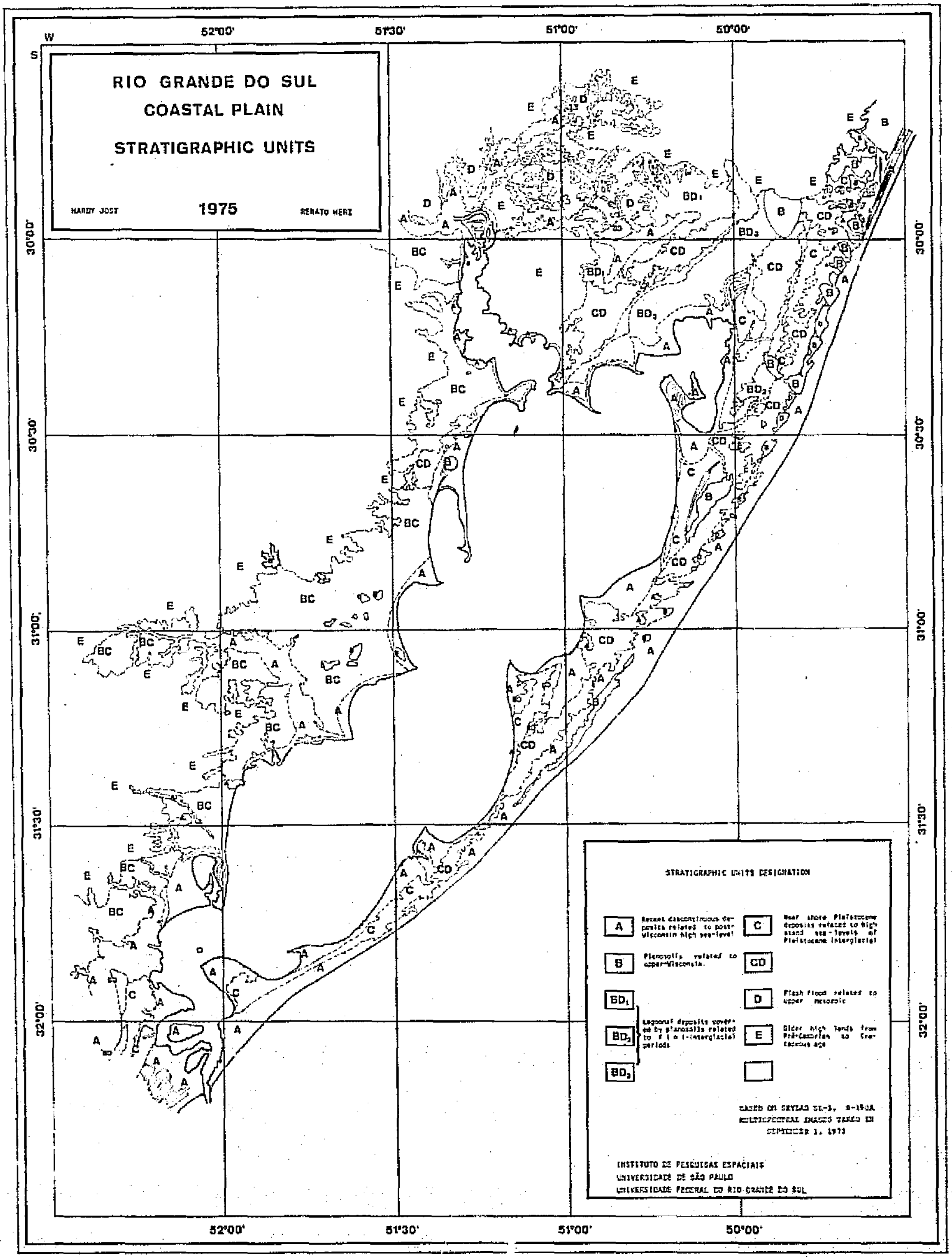
RIO GRANDE DO SUL
COASTAL PLAIN
STRATIGRAPHIC UNITS
HARDY JOST
1975
RENATO HERZ
52°00'
51°30'
51°00'
50°00'
30°00'
30°30'
31°00'
31°30'
32°00'
STRATIGRAPHIC UNITS DESIGNATION
INSTITUTO DE PESQUISAS ESPACIAIS
UNIVERSIDADE DE SÃO PAULO
UNIVERSIDADE FEDERAL DO RIO GRANDE DO SUL

a) beach-dune-ridges systems along beaches were located in paleogeographically favorable conditions to strong wave-action and regressive sand deposition.

b) drowned river-mouth deposits and deltaic evolution

c) peat bogs

d) wave and/or current built terraces

e) hanging beaches

2) Unit B

Planosols of upper-Wisconsin time developed on almost all older terrains of the coastal lowlands. Their high content in clay and silt favor their high impermeability and, for this reason, the preservation of a dense system of little lakes and ponds and marshes on top of it. Mammalian fossils found at some places at the base of these planosols showed an age of about 12,000 years B.C. (Jost & Soliani Jr., 1974). These planosols are cut by terraces against which the deposits corresponding to the Quinta transgression rest.

According to their occurrence, these planosols are referred to as two sub-units in Figure III.3, for interpretation purposes:

Sub-unit BC - In this case these planosols cover fluvial deposits, braided stream deposits, and mass movement deposits referred to tentatively as

Wisconsin low sea-level deposits, and which are known as the Graxaim Formation.

Sub-unit BD - In this case these planosols cover lagoonal deposits related to fini-interglacial periods. Three levels of occurrence were identified for this situation, designated as BD_1, BD_2, and BD_3 from the lower to the higher level, which probably means from the younger to the older level if we can consider that, during Pleistocene time, sea level fluctuations and lagoonal fluctuations reached lower altitudes from lower Pleistocene to upper Pleistocene age.

In both cases, this unit is known as the Cordão Soil Unit (Jost & Soliani Jr., op.cit.).

3) Unit C

Near-shore Pleistocene sand bar deposits known as Chui Formation, Taim Member (Jost, 1975), tentatively correlated to high stand sea levels of Pleistocene interglacial periods. In most places this unit is covered by partially eroded fossil sand dunes known as the Itapuã Formation (Delaney, 1965), newly re-defined to Itapuã Member of the Chui Formation (Jost, op. cit.). When covered by fossil dunes, the unit C takes the designation CD in Figure III.3.

4) Unit D

Flash flood, rill wash and gravel deposits of the Gravataí Formation (Morris, 1963), which represent correlative deposits of a retreating escarpment maintained by upper Mesozoic sedimentary and volcanic rocks.

5) Unit E

Older highlands ranging in age from pre-Cambrian to Cretaceous.

3.5.3 - Conclusions

In the foregoing analysis an attempt has been made to establish preliminary spectral evidences for Quaternary coastal geological mapping.

Considering the high volume of ground truth data collected during recent years, this first attempt to use orbital imagery over the test site in tracing regional delicate Quaternary features has proved to be very successful. In spite of the low linear resolution, it was possible to trace and to identify with great accuracy, the areal distribution of all known stratigraphic units. Simultaneous comparison with geological maps obtained from 1:60,000 aerial photographic interpretation showed that, for spacecraft imagery, the geometric fidelity favors better conditions for unit tracing. In the same way, it may be said that some

units were identified in the imagery and checked in the field in places where they had never been suspected of occuring.

As far as this preliminary interpretation of SKYLAB images in the test site permits the strong tonal variations of the major units permit identification and accurate delineation of detailed lithological units. In this way, all significant lithological units can be recognized in detail.

The use of multispectral orbital images for interpretation of the geomorphology and stratigraphical framework of coastal areas, as considered in the present paper, is a fertile field that has never been touched by investigators in Brazil for coastal studies and Quaternary Geology. We would like to suggest that the use of orbital multispectral images, as in the present results should be extended to the whole of the Brazilian coast where either morphological or geological units of Quaternary age are prominent.

3.6 - BIBLIOGRAPHY

DELANEY, P. J.V. - *Fisiografia e geologia de superfície e da planície costeira do Rio Grande do Sul* - UFRGS, Escola de Geologia, Publicação Especial nº 5, Pôrto Alegre, 1965.

HERZ, R. - *Orbital images and the possibility of studying hydrological and oceanographic resources of the Eastern regions of the state of Rio*

Grande do Sul, São José dos Campos, INPE. INPE-421-LAFE, 1973.

JOST, H. - "O Quaternário da Planície Costeira do Rio Grande do Sul" - *XXV Congresso Brasileiro de Geologia,* Anais, Vol. 1, pgs. 49-52, São Paulo, 1971.

JOST, H. & GODOLPHIM, M - "Holocene sea-levels in the Rio Grande do Sul Coastal plain, SE - Brazil" - *International Symposium on Quaternary,* Brazil, 1975 (in press).

JOST, H. & SOLIANI JR., E. - "A posição estratigráfica dos mamíferos pleistocênicos da província costeira do Rio Grande do Sul" In: *Congresso Argentino de Paleontologia e Bio-estratigrafia",* Tucuman, 1974. Anais (in press).

MORRIS, R. - *Geologia das folhas de Gravataí, Taquara e Rolante* - UFRGS, Escola de Geologia, Publicação especial nº 3., Pôrto Alegre, 1963.

NASA - *SKYLAB EARTH RESOURCES DATA CATALOG* - (JSC 09016) - Houston, Texas, 1974.

CHAPTER IV

UTILIZATION OF SKYLAB IMAGES IN PRECISION PROCESSING OF LANDSAT IMAGES

Prepared by:

José Carlos Maia

CHAPTER IV

UTILIZATION OF SKYLAB IMAGES IN PRECISION PROCESSING OF LANDSAT IMAGES

4.1 - TECHNICAL APPROACH AND TASK DESCRIPTION

The group named GEOS (Geodesy/Satellite) of the Institute of Space Research (INPE) is the group responsible for investigations on Geodesy, Cartography and Photogrammetry. For this reason we used SKYLAB images in a study of analytical aerotriangulation for determination of control points. We think these control points may be useful for derivation of precision images from bulk images of the LANDSAT satellite and for other cartographic activities.

4.2 - NARRATIVE HISTORY OF THE INVESTIGATION

Since the SKYLAB images have a forward overlap of 60%,they seem well suited to aerotriangulation work. Besides this, considering the necessity to establish many control points to support precision processing of LANDSAT images, we found that the SKYLAB images could be very useful for selection of control points.

In this way, we performed some experiments which can improve precision processing of LANDSAT images by means of more accurate control points.

4.3 - DISCUSSION OF THE TECHNIQUES AND PROCEDURES USED

4.3.1 - ANALYTICAL AEROTRIANGULATION

The control points (which are normally ground control points) to support the aerotriangulation of a test line were taken from 1:100,000 scale topographic maps. The instrumental coordinates of each one of those points were read in a Datagrid and transformed into ground coordinates by means of an affine transformation computer program.

In order to facilitate the identification of the points simultaneously on both LANDSAT and SKYLAB images, the later was enlarged to the scale of 1:1,000,000.

4.3.2 - INSTRUMENTAL PHASE

All the points of interest, after being marked on a paper collection image were transferred stereoscopically to the plates by means of a point transfer. The instrumental coordinates of each one of those points was determined by a monocomparator. In order to avoid gross errors, a criterion of forward and backward reading was established.

4.3.3 - COMPUTATIONAL PHASE

The computer programs: DATA EDIT, STRIP TRIANGULATION and

BLOCK ADJUSTMENT which normally come with Space Optic's Monocomparators, were adapted to our Burroughs B-6700 system to execute the desireable computations.

4.3.4 - ANALYTICAL TREATMENT OF THE INSTRUMENTAL COORDINATES

The mean values read in the comparator are computed by means of a computer program which punches a deck of cards for use in the DATA EDIT program.

As the coordinates read in the monocomparator are not considered to be precise enough for analytical triangulation their values must be refined, taking into account:

lens distortion
- film shrinkage
- atmospheric refraction, and
- Earth curvature

The DATA EDIT program is a check for operator and instrument errors. This program also punches a deck to be used in the next program.

The STRIP TRIANGULATION program, which is the next program to be used, performs the refinement of the coordinates, relative orientation, scaling of the models, and computation of strip coordinates for all the

models that form the strip and a diagnosis for gross errors. The last program to be used, the BLOCK ADJUSTMENT, computes the coeficients of the polynomial transformation by using the available ground control points and change points, and computes the ground coordinates for all points of interest.

4.3.5 - SUMMARY OF SKYLAB DATA FURNISHED

Black and white transparencies were utilized from station 5 of the Multispectral Photographic Camera, S190A, from the September 3,1973 SKYLAB SL-3 pass over eastern Brazil. Specific images used were frames 179-189, roll 35

4.3.6 - SUMMARY OF GROUND TRUTH ACTIVITIES

Because the test line was supported by control points taken from reliable 1:100,000 scale topographic maps, it was not necessary to carry out ground truth activities. However, ground checking will eventually be done for all precision images derived.

4.3.7 - PROBLEMS ENCOUNTERED

The only sources of problems were the scale limitation of the original film and cloud cover.

4.3.8 - RESULTS AND FINDINGS OF THE INVESTIGATION

Since the ground coordinates of the control points have not been determined directly in the field, the results of the test line seem satisfactory for determination of control points for precision processing of LANDSAT images. In order to reach desirable accuracy for systematic mapping, aerotriangulation must be supported by ground control points.

The root mean square errors obtained with the test line were in the order of 66 m, which is sufficiently accurate for precision processing of LANDSAT images.

CHAPTER V

SUMMARY OF RESULTS OBTAINED FROM THE ANALYSIS OF SKYLAB S192 CCT'S

Prepared by:

Eric Royer Stoner

CHAPTER V

SUMMARY OF RESULTS OBTAINED FROM THE ANALYSIS OF SKYLAB S192 CCT'S

5.1 - NARRATIVE HISTORY OF THE INVESTIGATION

In June 1975 the Brazilian Space Research Institute (INPE) obtained the IMAGE-100 Interactive Multispectral Image Analysis System from the General Electric Company. Shortly thereafter, work was begun to attempt to read video data from the SKYLAB S192 CCT's on the IMAGE-100 System.

5.2 - DATA FURNISHED

Computer Compatible Tapes from the August 8, 1973 pass of the SKYLAB SL-3 S192 multispectral scanner over southern Mato Grosso,Brazil (Fig. V.1) were obtained from the NASA Data Distribution Center. The eleven CCT's constitute S192 MSS output product number S051-2 and contain all 13 bands of spectral data as SDO's 1,3,5,7,9,11,13 and 17-22 (Table V.1). Data is in a line straightened format. Screening film of bands 2, 7 and 11 was provided in a five inch format.

5.3 - TECHNIQUES AND PROCEDURES USED

It was necessary to adapt a program whereby selections of

GMT Start Time: 16:22:54.053

GMT Stop Time: 16:23:59.459

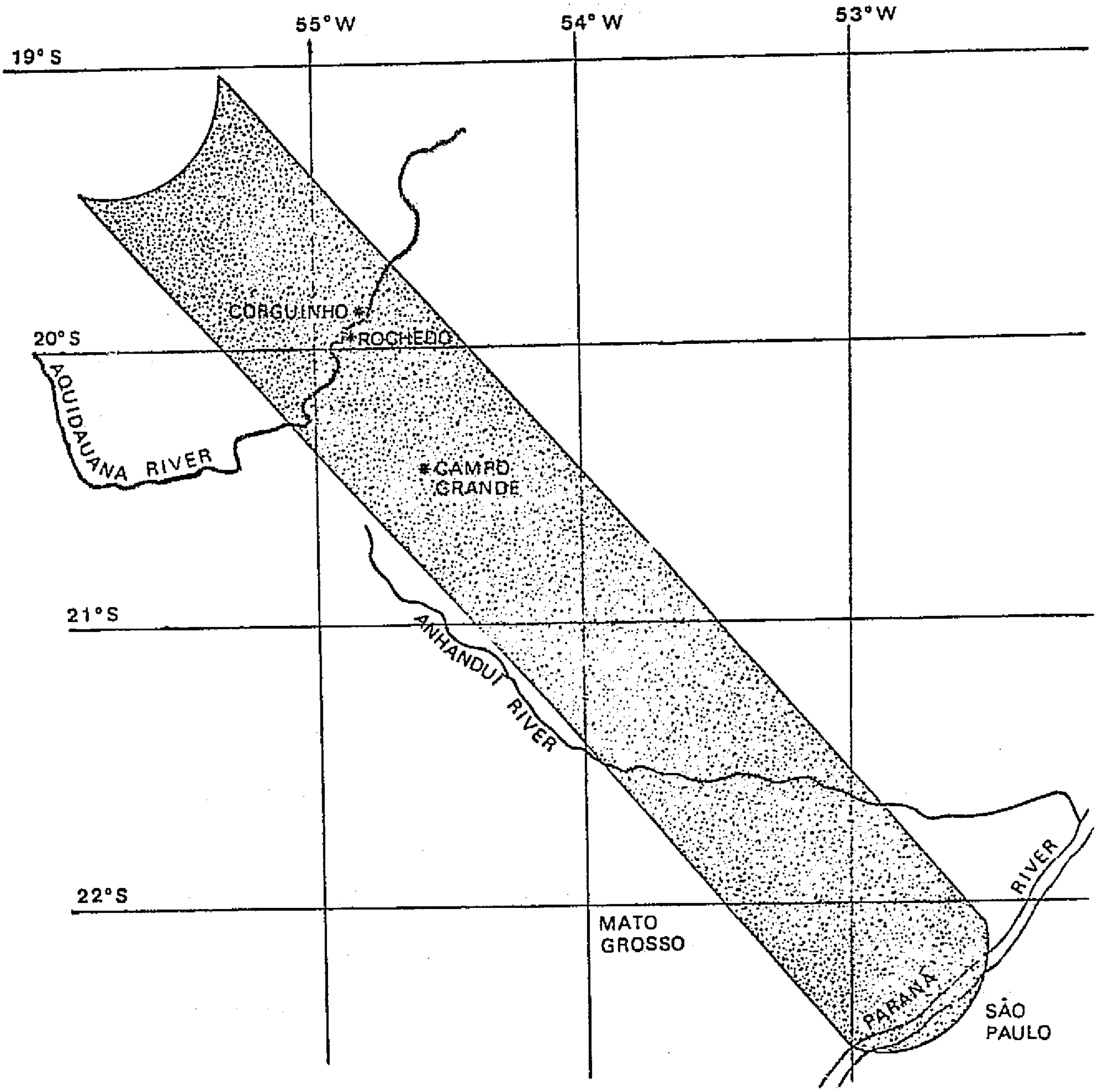

Fig. V.1 - Location of August 8, 1973 SKYLAB-3 S192 MSS pass over Southern Mato Grosso, Brazil.

TABLE V.1

CCT's AVAILABLE FROM AUGUST 8, 1973 SKYLAB SL3

MSS PASS OVER SOUTHERN MATO GROSSO, BRAZIL

TAPE Nº	SKYLAB SL3 EREP ACCESSION Nº	TAPE SEQUENCE	TIME SLICE	GMT START/STOP TIME	
924661	33-22329	1 of 3	1	220:16:22:54.0192	start
924662	33-22330	2 of 3	1		
924663	33-22331	3 of 3	1	220:16:23:13.9992	stop
924664	33-22332	1 of 3	2	220:16:23:10:0016	start
924665	33-22333	2 of 3	2		
924666	33-22334	3 of 3	2	220:16:23:29.9924	stop
924667	33-22335	1 of 3	3	220:16:23:26.0046	start
924668	33-22336	2 of 3	3		
924669	33-22337	3 of 3	3	220:16:23:45.9955	stop
924670	33-22338	1 of 2	4	220:16:23:42.0085	start
924671	33-22339	2 of 2	4	220:16:23:58:9929	stop

not more than 5 bands of the 13-band CCT's were read at one time, due to the memory limitation of the IMAGE-100 System (specially designed to analyze 4-band LANDSAT imagery).

A program was developed which succeeded in reading the 13 bands of video data contained on the S192 CCT's. Any combination of five or fewer bands can be stored in the memory at any given time. Reading every data point of the S192 scanner imagery, it is possible to display a swath of 512 lines by 512 samples on the color CRT display representing more than one-third of the 1240 sample data block. A center swath can be read by beginning to read data on the 365th sample. Any portion of the CCT can be read at the normal sampling rate, or can be sampled by reading every other line and sample within the line enabling most of the data block to be read at the same time. Ancillary block information is printed out on a line printer for selected scan lines, indicating latitude and longitude of the left, center, and right data points as well as time at the start of the data set and spacecraft altitude.

5.4 - PROBLEMS ENCOUNTERED AND THEIR RESOLUTION

Original difficulties in reading data from the seven data records and in reading the end-of-file were overcome, allowing the 13 SDO's on the CCT to be separated for display on the color CRT of the IMAGE-100 System. Initial confusion as to the SDO/band assignments occurred because of the similarity of sensor band 11 and 12 imagery to visible imagery.

Lack of good quality data in the visible bands further complicated positive sensor band identification. Additional consideration of the plant and soil spectral properties of the study area, at this time of the year, led to the realization that bands 11 and 12 were correctly identified as non-photographic IR bands beyond the 1.45 μm water absorption region.

Image distortion on the left and right extremes of the imagery presents a serious limitation to the recognition of ground features. The central portion of the imagery has only slight distortion, however, and is quite suitable for multispectral analysis using automatic data processing.

5.5 - RESULTS AND FINDINGS

Data quality of the 13 bands of the SKYLAB S192 MSS varied considerably (Table V.2 and Fig. V.2). The August 8, 1973 pass over Southern Mato Grosso was practically cloud-free (although haze and smoke were present) and presented a variety of ground features of interest, including: native and planted grasslands (some of which were burning at the time of the pass), forest and scrub forest ("cerrado") vegetation, reforested areas, humid lowlands, and limited areas of agricultural exploration. Knowledge of the spectral response of these ground features from SKYLAB S190B photography and LANDSAT images aided in evaluation of the SKYLAB S192 MSS imagery.

In general, the visible bands are of poor quality due to noise problems or low contrast imagery. Band 1 (violet)contains no image,

TABLE V.2

EVALUATION OF IMAGE QUALITY FOR 13 BANDS OF THE SKYLAB S192 MSS VIEWED ON THE IMAGE-100 SYSTEM

SKYLAB S192 MSS BAND DESCRIPTION	WAVELENGTH REGION	APPEARANCE OF IMAGERY ON IMAGE-100 COLOR CRT DISPLAY
1 (violet)	0.41-0.46 μm	no image
2 (violet-blue)	0.46-0.51 μm	poor quality, hazy, very low contrast
3 (blue-green)	0.52-0.56 μm	poor quality, low contrast
4 (green-yellow)	0.56-0.61 μm	fair quality, noisy
5 (orange-red)	0.62-0.67 μm	poor quality, very noisy
6 (red)	0.68-0.76 μm	good quality, but not a true visible band
7 (near IR)	0.78-0.88 μm	good quality
8 (near IR)	0.98-1.08 μm	good quality
9 (near IR)	1.09-1.19 μm	good quality
10 (near IR)	1.20-1.30 μm	good quality
11 (middle IR beyond the 1.45μm H_2O absorption region)	1.55-1.75 μm	very good quality
12 (middle IR beyond the 1.45μm H_2O absorption region)	2.10-2.35 μm	very good quality
13 (Thermal IR)	10.20-12.50μm	fair quality

Fig. V.2 - SKYLAB S192 MSS image displayed on the IMAGE-100. From SL3 CCT, accession no. 33-22330, August 8, 1973, region of Rio Aquidauana, Mato Grosso state, Brazil.

Fig. V.2 (continued). SKYLAB S192 MSS image displayed on the IMAGE-100 System. From SL3 CCT, accession no. 33-22330, August 8, 1973, region of Rio Aquidauana, Mato Grosso State, Brazil.

while band 2 (violet-blue) presents very low contrast. Contrast is also low in band 3 (blue-green). Smoke plumes from rangeland fires and land clearing operations are evident in bands 2 and 3. Bands 4 (green-yellow) and 5 (orange-red) have serious noise problems, although band 4 is perhaps the best of the visible bands. Band 6 (red) is of good quality, but is more of an IR band than a visible one (wavelength band 0.68-0.76 μm). Bands 7,8,9 and 10 (near IR) are of good quality and are quite useful for delimitation of burned areas. Bands 11 and 12 (middle IR beyond the 1.45 μm water absorption band) contain excellent imagery and can at first sight be interpreted as visible images, although further investigation reveals the unique spectral properties of this IR wavelength region. Interestingly, the foci of numerous fires are distinctly visible in bands 11 and 12. Band 13 (thermal IR) is of fair quality and seems to be most useful in identifying the gallery forests (cooler areas) and burned-over areas (hotter areas).

Image quality on the IMAGE-100 System is quite superior to that of the five inch screening film provided by NASA. Imagery displayed on the IMAGE-100 color CRT appears to be less distorted, and contains much better ground resolution than in the screening film.

Ability to analyze the 13 band SKYLAB S192 MSS imagery on the IMAGE-100 System has provided a useful step in an integrated system involving automatic data processing of orbital imagery for land resource mapping.

CHAPTER VI

FEATURE SELECTION ALGORITHM

Prepared by:

Ravindra Kumar

CHAPTER VI

FEATURE SELECTION ALGORITHM

6.1 - INTRODUCTION

One of the problems commonly encountered in pattern recognition is the selection of effective features from a given set of measurements. The use of a large number of feature measurements increases the complexity, the size and the computer time required by the classifier (Swain, 1972). For example, in the remote sensing of earth resources and environment, the problem reduces down to the following. Given a set of N features (e.g. multispectral scanner channels), find a subset consisting of n channels which provides an optimal trade off between classification cost and classification accuracy (Fu, 1970). For example, SKYLAB multispectral scanner (S192) has 13 channels and generally an analyst wants to use the best four or five of these channels for classification.

The effectiveness of the features should be determined by performance of the recognition system, usually in terms of probability of correct recognition. Ideally, one would like to solve this problem by computing the probability of misclassification associated with each n feature subset and then selecting the one giving best performance (Swain, 1972). However, it is generally not feasible to perform the required computations. Even when one assumes normal distribution, numerical integration

is required which in the multidimensional case is impractical to carry out. Some of the techniques of feature selection are summarized below.

6.2 - FEATURE SELECTION TECHNIQUES

Fu (1970) has used a non-parametric feature selection technique based on the direct estimation of error probability. The proposed feature selection criterion was based on the direct estimation of the minimized probability of misclassification from a given set of training samples. Maximum likelihood decision rule (MLDR) was used for classification. He pointed out that a large amount of computation time is required especially when the number of classes is large. Using 7530 test samples, he applied the proposed nonparametric method of feature selection to crop classification. The results of his experiment are given in Table VI.1. He found that all the classes are separable for most 4-feature subsets (41 sets).

Many authors have studied the linear feature-space transformation techniques to apply for the feature selection problems. For example, Watanabe (1966) introduced the feature-space compression technique based on Karhunen-Loeve (K-L) expansion. Fu (1971) tested the feature selection technique based on generalized K-L expansion on crop classification. The results were compared with those using parametric feature selection technique. The MLDR was used for the classifier and the appropriate statistical parameters were estimated from training samples for each class. He found that the transformed p-dimensional feature space was less effective than the

TABLE VI.1

RESULTS OF NONPARAMETRIC FEATURE SELECTION TECHNIQUE

NONPARAMETRIC METHOD			PARAMETRIC METHOD	
NUMBER OF FEATURES	BEST FEATURE SET	PERCENT ERROR	BEST FEATURE SET	PERCENT ERROR
1	x_9	33.8	x_9	37.6
2	x_1, x_9	3.1	x_i, x_9	10.6
3	x_1, x_{10}, x_{11}	0.1	x_1, x_{10}, x_{11}	5.0
	x_1, x_9, x_{12}			
4	41 - feature set	0.0	x_1, x_6, x_{10}, x_{11}	4.9

same dimensional feature subspace for all P ($\leq N$ = total number of available features), but the difference in performance for the 4-feature subset was only 1.3 percent. The computation time required, on the other hand, is much shorter for the transformation technique.

An intermediate quantity which is related to the classification accuracy is often used as a basis for feature selection (Fu, 1971). Divergence between pattern classes has been proposed as a criteria for feature selection. The application of divergence as a criterion for feature selection is briefly introduced in the following.

Divergence is defined in terms of the likelihood ratio $L_{ij}(X) = \frac{P(X|\omega_i)}{P(X|\omega_j)}$ which is a measure or indication of the separability of the densities at $\bar{x}$. The logarithm of the likelihood ratio also provides a measure of separability of the densities (Kullback, 1959).

$$\text{Let } L'_{ij}(X) = \log L_{ij}(X) = \log P(X|\omega_i) - \log (X|\omega_j) \tag{1}$$

Divergence is defined as

$$D(i,j,]c_1, c_2 \ldots\ldots\ldots c_n) = E\left[L^1_{ij}(X)\middle|\omega_i\right] - E\left[L^1{}_{ij}(x)\middle|\omega_j\right] \tag{2}$$

for channels c_1, c_2 .... c_n where

$$E\left[L^1_{ij}\ (x)\middle|\omega_i\right] = \int_X L^1_{ij}(x)\quad P(X|\omega_i)dx$$

Divergence is defined for any two density functions. In the case of normal variables with unequal covariance matrices, it can be shown (Kailath, 1967) that $D(i,j|c_1,c_2 \ldots\ldots c_n) = \frac{1}{2}\,\mathrm{tr}\left[(\Sigma_i-\Sigma_j)(\Sigma_j^{-1} - \Sigma_i^{-1})\right] +$

$$+\frac{1}{2}\mathrm{tr}\left[(\Sigma_i^{-1} + \Sigma_j^{-1})\ (U_i - U_j)\ \ (U_i - U_j)^T\right] \tag{3}$$

It can be shown that the probability of misclassification is a monotonically decreasing function of divergence. Therefore features selected according to the magnitude of divergence will imply their corresponding discriminatory power between the classes i and j. In other words, feature set α_p is considered more effective than the feature set α_ℓ if $D(i,j|\alpha_p) > D(i,j|\alpha_\ell)$ (Fu, 1970). Divergence is a distance measure between the two statistical distributions. It is an indirect measure of the ability of the classifier to successfully discriminate between them.

Divergence has the following properties (Swain, 1972).

1) $D(i,j\ |c_1,\ldots, c_n) > 0$ for non-identical distributions

2) $D(i,i\ |c_1,\ldots,c_n) = 0$

3) $D(i,j\ |c_1,\ldots,c_n) = D(j,i\ |\ c_1,c_2,\ldots c_n)$

4) Divergence is additive for independent features

$$D(i,j\ |c_1,c_2,\ldots,c_n) = \sum_{k=1}^{n} D(i,j\ |\ c_k)$$

5) Adding new features never decreases the divergence, i.e.,
$D(i,j \mid c_1,\ldots,c_n) \leq D(i,j \mid c_1,\ldots c_{n+1})$

Fu (1970) assumed that feature vectors for each class were gaussianly distributed. He used the linear classification procedure based on the maximum likelihood decision rule (MLDR) for multiclass classification problem by means of minimizing the maximum probability of overall misclassification (minimax procedure, Anderson and Bahadue, 1962).

He showed that a monotonic functional relationship exists between the probability of pairwise misclassification between the classes and the separability measure. In addition, he showed that in the case of Gaussianly distributed pattern classes with equal covariance matrices, the divergence and the separability measure have a monotonic relationship. Nevertheless it is clear that the separability measure is a more general criterion for feature effectiveness. He tested the effectiveness of the feature sets by computing the percentage of misclassification with 7530 test samples (approximately 1500 samples per class) classified by MLDR classifier. He selected the optimum feature sets from all possible combinations. He found from experimental results that it is possible for smaller size feature subsets to be almost as effective as the complete feature set. Thus, in many situations selecting optimum feature subset considerably reduces the computer time required for classification as compared to using the entire feature set with a relatively small loss of classification accuracy.

Although divergence only provides a measure of the distance between two class densities, its use is extended to the multiclass case by taking the average over all class pairs (Fu, 1971).

If D_{ij} is the divergence between classes i and j, then the multiclass feature selection criterion is

$$D_{AVE} = \frac{2}{m(m-1)} \sum_{i=1}^{m-1} \sum_{j=i+1}^{m} D_{ij} \tag{4}$$

Another strategy is to maximize the minimum pairwise divergence (Grettenberg, 1963; Fu and Chen, 1969; Kodota and Shepp, 1967; Swain, 1972) i.e., to select the feature combination which does the best job of separating the hardest to separate pair of classes, i.e., for example consider a situation where there are 3 classes A, B and C

$$D_{MIN} = \text{Min}\ \{D_{AB}, D_{BC}, D_{CA}\} \tag{4A}$$

Where D_{AB} = divergence between class A and class B

The relationship between the divergence and classification accuracy is highly nonlinear (in fact, divergence increases without bound as the class separability increases, whereas probability of correct classification must saturate at 100 percent), and it is found that widely separable classes make too much of a contribution to D_{AVE} as compared with less separable classes.

As a result, in problems involving a wide range of class separabilities, D_{AVE} is not a reliable criterion for feature selection. This is illustrated in Figure VI.1.

On the other hand, D_{MIN} is based on selecting the channels which do the best job of separating the hardest-to separate pair of classes. Although this is certainly a reasonable strategy in many remote sensing problems, there is no guaranty that it is the optimal one. This is illustrated in Figure VI.2.

As pointed out before, as the separability of a pair of classes increases, the pairwise divergence also increases without limit but the probability of correct classification saturates at 100 percent. A modified form of divergence, referred to as the "transformed divergence", D has a behavior more like the probability of correct classification than divergence (Swain, 1973).

$$D_T = 2 \left[1 - \exp(-D18)\right] \tag{5}$$

where D is the divergence discussed above. The saturating behavior of this function reduces the effects of widely separated classes when taking the average over all pairwise separations. D_{AVE} based on transformed divergence has been found a much more reliable criterion for feature selection than D_{AVE} based on "ordinary" divergence.

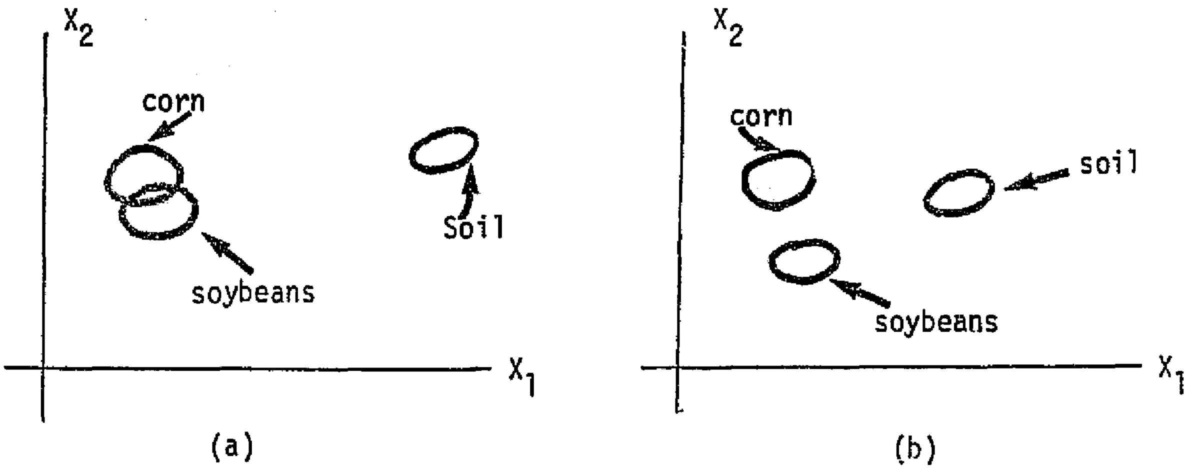

Although D_{AVE} would be larger in (a), overall classification accuracy may be better for the situation in (b).

Fig. VI.1 - Disadvantage of D_{AVE}. (Taken from Swain (1972)).

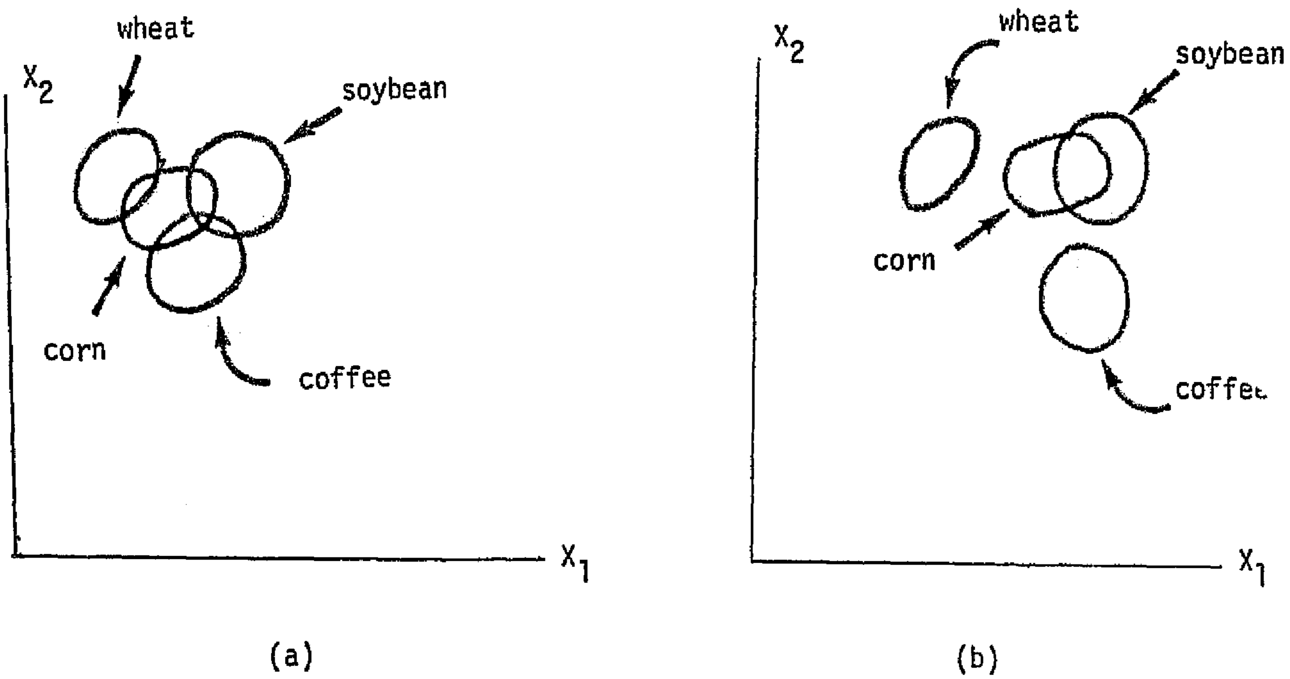

Although D_{MIN} would be larger in (a), overall classification accuracy may be better for the situation in (b).

Fig. VI.2 - Disadvantage of D_{MIN}.

VI.3 - COMPARISON OF FEATURE SELECTION TECHNIQUES

Swain et al. (1971) have shown experimentally that a separability measure referred to as the Jeffreys-Matusita Distance (JM-distance) provides a much more reliable criterion than divergence, presumably because as a function of class separability it behaves more like probability of correct classification. For two densities $p_1(x)$ and $p_2(x)$, the JM-distance J is given by

$$J = \int_X \left[\sqrt{P_1(x)} - \sqrt{P_2(x)} \right]^2 dx \qquad (6)$$

which can also be written in the form

$$J = 2(1-\rho), \text{ where } \rho = \int_X \sqrt{P_1(X)P_2(X)}\ dx \qquad (7)$$

If $P_i(x)$, i=1,2 are multivariate Gaussian densities as above then $\rho = e^{-\alpha}$ and $J = 2\,(1 - e^{-\alpha})$, where $\alpha = \frac{1}{8}(U_1 - U_2)^T\, \Sigma^{-1}\, (U_1 - U_2) +$

$$+ \frac{1}{2} \log_e \left[\frac{\det \Sigma}{\left[\det.\ \Sigma_1 .\ \det \Sigma_2\right]^{1/2}} \right]$$

$$\text{and } \Sigma = \frac{1}{2}\left[\Sigma_1 + \Sigma_2\right] \qquad (8)$$

In eq. (8), det A means the determinant of matrix A. Since $0 \le e^{-\alpha} \le 1$, J ranges from 0 to 2 with 2 corresponding to the largest separation. It was observed by Swain et al. that this "saturating" behavior

of J is responsible for its utility as a feature selection criterion in multiclass problems. JM-distance and divergence are related by the inequality

$$J \leq 2 \left[1 - \exp\,(-D/8)\right] \tag{9}$$

or $J \leq D_T$ (see eq. (5)), where $D_T = 2\left[1 - \exp(-D/8)\right]$

Swain and King (1973) performed an experiment to compare the separability measures divergence, transformed divergence and JM distance. Based on typical second order statistics derived from real remote sensing data, 2790 sets of Gaussianly distributed artificial data were generated; each set contained 1000 observations for each of two pattern classes in a feature space of dimensionality ranging from 1 to 6 (465 sets were generated for each dimension 1,2,...6). For each set the divergence, transformed divergence and JM distance were computed, and the actual classification error for the 2000 observations was taken as the associated probability of error. The results are summarized in Figures VI.3 to VI.5. It shows that both transformed divergence and J-M distance are much better measures for feature selection than divergence. In addition JM distance is a slightly better measure of feature selection as compared to the transformed divergence because of the following reasons (Swain et al. 1973).

1) JM distance is a little better than transformed divergence in predicting classification accuracy.

Fig.VI.3* - Probability of Correct Classification (P_c) vs. JM-Distance (J).

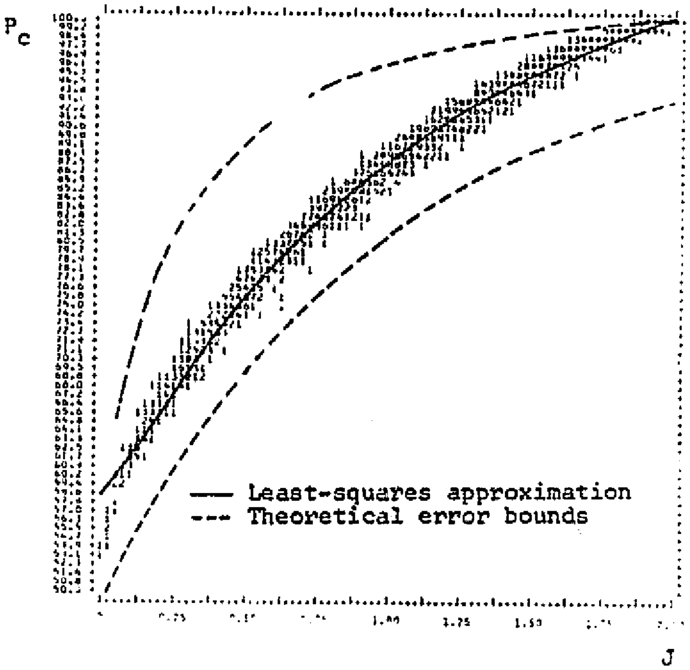

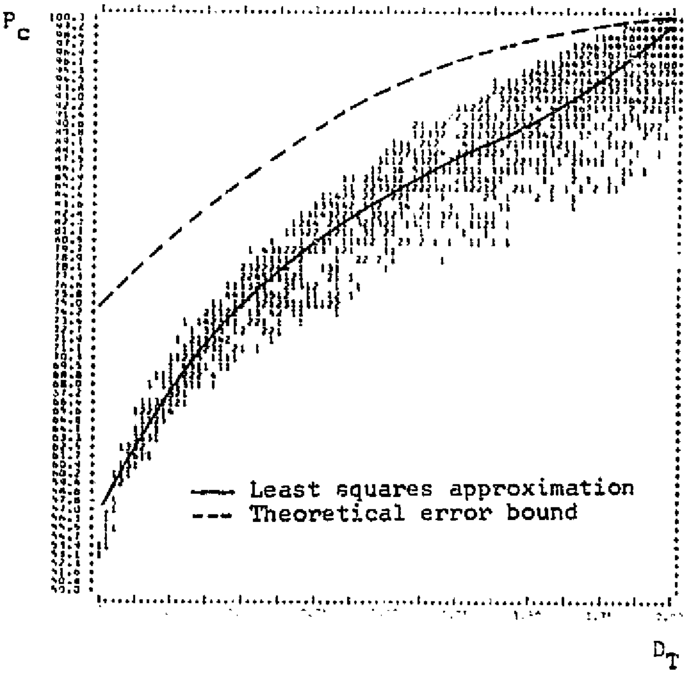

Fig. VI.4* - Probability of Correct Classification (P_c) vs. Transformed Divergence (D_T).

Fig.VI.5* - Probability of Correct Classification (P_c) vs. Divergence (D).

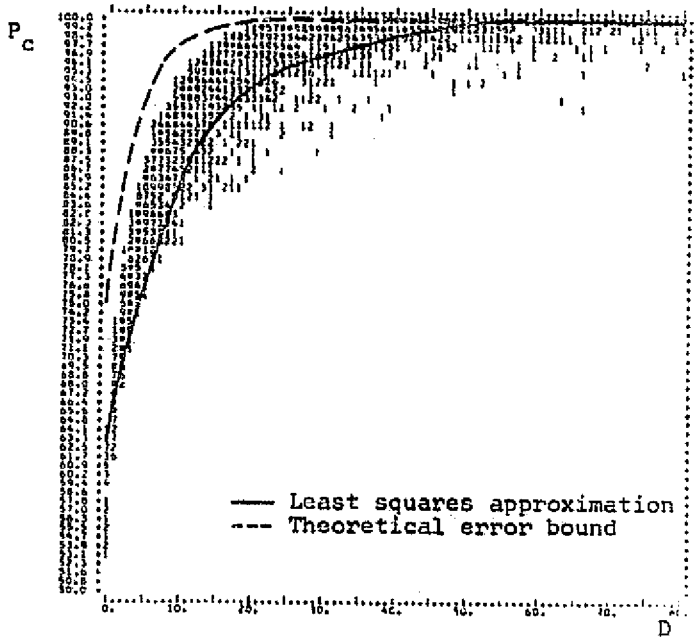

---

* These figures are taken from Swain & King (1973).

2) There is much tighter clustering of the experimental results about the regression curve for the case of JM-distance so that performance is "much more predictable" as a function of JM-distance.
3) There is a lower bound on classification accuracy as a function of JM-distance; no such lower bound is available for transformed divergence.

VI.4 - FEATURE SELECTION ALGORITHM OF INPE

At the "Instituto de Pesquisas Espaciais - INPE" a subroutine has been developed to compute mean vector, covariance matrix and JM distance between any two given classes.

In addition, a subroutine has been prepared which reads the computer compatible tapes of Multispectral Scanner (S192) of SKYLAB. It can store and display ten channels, five on the top half of the display of IMAGE-100* of General Electric and five on its bottom half. In addition it performs the following functions.

1) Compute the weighted average JM distance averaged over all pairs of classes, i.e.,

$$J_{AVE} = \frac{\sum_{i=1}^{m-1} \sum_{j=i+1}^{m} \omega_{ij} J_{ij}}{\sum_{i=1}^{m-1} \sum_{j=i+1}^{m} \omega_{ij}} \tag{10}$$

---

* *IMAGE-100 is a Data Processing System for analyzing the earth resources data. It extracts thematic information and enhances the image.*

where m = no. of classes and ω_{ij} is the weight for discriminating class i from class j. ω_{ij} is selected by the analyst depending upon the importance he gives for discriminating class i from class j. If all the weights ω_{ij} are taken equal to one, eq. (10) reduces to

$$J_{AVE} = \frac{2}{m(m-1)} \sum_{i=1}^{m-1} \sum_{j=i+1}^{m} J_{ij} \tag{11}$$

If an analyst is not interested in discriminating certain pairs of classes, the weights, ω_{ij}, for those pairs can be taken equal to zero.

2) Compute the minimum JM distance over all pairs of classes, i.e.,

$$J_{MIN} = \underset{\substack{i=1 \text{ to } m-1 \\ j=i+1 \text{ to } m \\ i \neq j}}{\text{Min}} \{J_{ij}\} \tag{12}$$

J_{ij} is a vector and Min $\{J_{ij}\}$ denotes the element of the vector having the least value. If certain pairs of classes are not of interest to the analyst, those could be deleted from the analysis.

3) Print first R combinations of n (n is an integer lying between 1 and 5) channels out of 10 available channels in the descending order of J_{AVE} (see eq. (10)), i.e. print the combination of channels having the highest value of J_{AVE} first, print the combination of channels having the second highest value of JM distance second ..., print the combination having the least value of JM distance last. R is selected by the user.

For example, a user may like to see 20 combinations of 4 channels in the descending order of J_{AVE}. The value of n is also selected by the user. Similarly it can print R combinations of n channels out of 10 available channels in the descending order of JM_{MIN} (see eq. (12)).

This algorithm was tested on an artificially generated data. It was verified that it calculates the value of mean vector, covariance matrix, JM distance etc. correctly. In addition, this algorithm was used to select the best on the criterion of maximizing the JM distance between the classes of water and bare soil using the computer compatible tape of S192 scanner of SKYLAB (Input tape no. 921583, date 10.11.74).

VI.5 - BIBLIOGRAPHY

ANDERSON, T.W. AND BAHADUE, R.R. - *Classification into Two Multivariate Normal Distributions with Different Covariance Matrices* , Ann. Math. Stat., Vol.33, pp.420-431, 1962.

FU, K.S. AND CHEN, C.H. - *Sequential Decisions, Pattern Recognition and Machine Learning*. Tech. Rept. TR-EE 65-5, School of Electrical Engineering, Purdue University, Lafayette, Ind., 1969.

FU, K.S. - *Feature Selection in Pattern Recognition*. IEEE Trans. Syst., Sci. & Cybern; SSC-6(1): 33-39, 1970.

FU,K.S. - *On the Application of Pattern Recognition Techniques to Remote Sensing Problems*.TR-EE-71-13, School of Electrical Engineering,Purdue University, W.Lafayette, Ind., 91p.,1971.

GRETTENBERG, T.L. - *Signal Selection in Communication and Radar Systems*. IEEE Trans. Information Theory, vol. IT-9:265-275,1963.

KADOTA, T.T. AND SHEPP, L.A. - *On the Best Finite Set of Linear Observables for Discriminating two Gaussian Signals*. IEEE Trans. Information Theory, vol. IT13:278-284,1967.

KAILATH, T. - *The Divergence and Bhattacharyya Distance Measures in Signal Selection* . IEEE Trans. Comm. Tech., COM-15(1):52-60,1967.

KULLBACK, S. - *Information Theory and Statistics*,Wiley, New York, 1959.

SWAIN, P.H., ROBERTSON, T.V.,AND WACKER, A.G. - *Comparison of the Divergence and B-Distance in Feature Selection*. LARS Information Note 020871, Laboratory for Applications of Remote Sensing, Purdue University, W. Lafayette, Indiana, 1971.

SWAIN,P.H. - *Pattern Recognition: A Basis for Remote Sensing Data Analysis.* LARS Information Note 111572, Laboratory for Applications of Remote Sensing, Purdue University, W. Lafayette, Indiana, 40p.,1972.

SWAIN, P.H. AND KING, R. C. - *Two Effective Feature Selection Criteria for Multispectral Remote Sensing.* Presented at the International Joint Conference on Pattern Recognition, Washington, D.C., Nov. 1973.

WATANABE, S - *A Method of Self-Featuring Information Compression in Pattern Recognition.* Proc. Bionics Symp., 1966.

CHAPTER VII

RECOMMENDATIONS OF THE PRINCIPAL INVESTIGATOR

CHAPTER VII

RECOMMENDATIONS OF THE PRINCIPAL INVESTIGATOR

Data of SKYLAB has demonstrated its value for many of the earth resources applications where finer resolution radiometrically calibrated data in several spectral channels is needed to complement the interpretation done using LANDSAT data.

On the other hand, in the attempts made to acquire SKYLAB data in a systematic way to obtain area coverages the problem of cloud cover appears to be a disturbing factor for certain regions of the world, as is case in several areas of Brazil.

Taking into account the flexibility of operation which will be provided by the Shuttle in the future, in connection with manned SKYLAB-type orbital craft, it is suggested that instead of attempting area coverage by them, which will still be provided by LANDSAT craft, manned orbital vehicle be used to collect earth resources data from specific spots as selected by researchers from previous studies and interpretation of LANDSAT data.

This might contribute to a better efficiency in the utilization of the necessarily limited time of manned missions.

APPENDIX A

AVAILABLE SKYLAB MAG TAPES

S-191 INFRARED SPECTROMETER

ACCESSION NO	TAPE NO	DATE
33-02510	906328	1/12/73
33-02511	906329	1/12/73
33-02538	906336	1/12/73
33-02539	906337	1/12/73
33-12968	916499	16/06/74
33-12969	916500	16/06/74
33-12966	916501	16/06/74
33-12967	916502	16/06/74

S-192 MULTISPECTRAL SCANNER

ACCESSION NO	TAPE NO	DATE
32-02803	906668	10/12/73
32-02893	907255	20/12/73
33-22329	924661	11/10/74
33-22330	924662	11/10/74
33-22331	924663	11/10/74
33-22332	924664	11/10/74
33-22333	924665	11/10/74
33-22334	924666	11/10/74
33-22335	924667	11/10/74
33-22336	924668	11/10/74
33-22337	924669	11/10/74
33-22338	924670	11/10/74
33-22339	924671	11/10/74
33-22364	926346	28/10/74
33-22365	926347	28/10/74
33-22366	926348	28/10/74
33-22367	926349	28/10/74
33-22368	926350	28/10/74
33-22369	926351	28/10/74
33-22370	926352	28/10/74
33-22371	926353	28/10/75

S-192 MULTISPECTRAL SCANNER (Cont.)

ACCESSION Nº	TAPE Nº	DATE
33-22372	926354	28/10/74
33-22373	926355	28/10/74
33-22374	926356	28/10/74
33-22363	926357	28/10/74
33-22448	929609	2/12/74
33-22449	929610	2/12/74
33-22450	929611	2/12/74
33-22451	929612	2/12/74
33-22452	929613	2/12/74
33-22453	929614	2/12/74
33-22454	929615	2/12/74
33-22455	929696	2/12/74
33-22456	929617	2/12/74
33-22457	929618	2/12/75
33-22458	929619	2/12/75
33-22459	929620	2/12/74
33-22460	929621	2/12/74
33-22461	929622	2/12/74
33-22462	929623	2/12/74
33-22463	929624	2/12/74
33-22464	929625	2/12/74
33-22465	929676	2/12/74
33-22466	929677	2/12/74
33-22467	929678	2/12/74
33-22468	929679	2/12/74
33-22469	929680	2/12/74
33-22470	929681	2/12/74
33-22471	929682	2/12/74
33-22472	929683	2/12/74
33-22473	929577	3/12/74
33-22719	933259	21/01/75
33-22720	933260	21/01/75
33-22723	933261	21/01/75
33-22724	933262	21/01/75
33-22725	933263	21/01/75
33-22726	933264	21/01/75
33-22727	933265	21/01/75
33-22728	933275	21/01/75
33-22729	933276	21/01/75
33-22730	933277	21/01/75
33-22721	933514	21/01/75
33-22722	933515	21/01/75

S-193 RADIOMETER-SCATTEROMETER-ALTIMETER

ACCESSION Nº	TAPE Nº	DATE
32-02653	903654	16/10/73
32-02652	903657	16/10/73
32-02913	909087	08/01/74
32-02909	909088	08/01/74
33-12242	909442	08/01/74
33-12245	909468	08/01/74
33-12259	909481	08/01/74
33-12297	909482	08/01/74
33-12298	909483	08/01/74
33-12243	909484	08/01/74
33-12260	909485	08/01/74
33-12264	909498	17/01/74
33-12296	909523	17/01/74
33-12580	909735	17/01/74
32-12648	927375	07/11/74
32-12649	927376	07/11/74
33-22720	933240	21/01/75
33-22808	933950	21/01/75
33-22808	933950	10/02/75
33-22810	933951	10/02/75
33-22811	933952	10/02/75
33-22812	933953	10/02/75
33-22849	934025	13/02/75
33-22720	934028	13/02/75
33-22845	934029	13/02/75
33-22846	934030	13/02/75
33-22847	934031	13/02/75
33-22848	934032	13/02/75
33-22842	934033	13/02/75
33-22843	934034	13/02/75

S-194 L-BAND RADIOMETER

32-02793	903331	13/10/73
32-02643	904214	26/10/73
33-02730	904559	31/10/73
33-02072	904560	31/10/73
33-02083	904650	02/11/73
33-02268	904859	05/11/73
33-02267	904860	05/11/73
33-02269	904863	05/11/73
33-12666	909835	24/01/74
33-22125	917181	28/06/74

S-194 L-BAND RADIOMETER (Cont.)

ACCESSION Nº	TAPE Nº	DATE
33-22114	917185	28/06/74
33-22127	917188	28/06/74
33-22129	917197	28/06/74
33-22115	917204	28/06/74
33-22116	917205	28/06/74